

AD-A087 105

SCHOOL OF AEROSPACE MEDICINE BROOKS AFB TX F/G 6/18
LASER RAMAN SPECTROSCOPY OF ULTRAVIOLET-INDUCED CATARACTS IN RA--ETC(U)
DEC 79 D M THOMAS, K L SCHEPLER
UNCLASSIFIED SAM-TR-79-40

NL

1 of 1
AD-A087 105

END
DATE
FILMED
9-80
DTIC

Report SAM-TR-79-40

LEVEL II

2

ADA 087105

**LASER RAMAN SPECTROSCOPY OF
ULTRAVIOLET-INDUCED CATARACTS
IN RABBITS AND MONKEYS**

Dwaine M. Thomas, Ph.D.

Kenneth L. Schepler, Captain, USAF

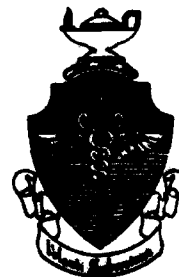
DTIC
JUL 24 1980
D

December 1979

Final Report for Period September 1977 - February 1979

Approved for public release; distribution unlimited.

USAF SCHOOL OF AEROSPACE MEDICINE
Aerospace Medical Division (AFSC)
Brooks Air Force Base, Texas 78235



DDC FILE COPY

80 7 21 07

NOTICES

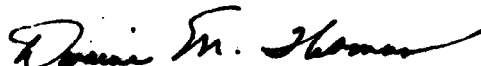
This final report was submitted by personnel of the Laser Effects Branch, Radiation Sciences Division, USAF School of Aerospace Medicine, Aerospace Medical Division, AFSC, Brooks Air Force Base, Texas, under job order 7757-02-53.

When U.S. Government drawings, specifications, or other data are used for any purpose other than a definitely related Government procurement operation, the Government thereby incurs no responsibility nor any obligation whatsoever; and the fact that the Government may have formulated, furnished, or in any way supplied the said drawings, specifications, or other data is not to be regarded by implication or otherwise, as in any manner licensing the holder or any other person or corporation, or conveying any rights or permission to manufacture, use, or sell any patented invention that may in any way be related thereto.

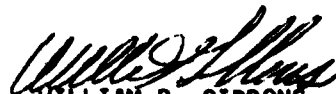
The animals involved in this study were procured, maintained, and used in accordance with the Animal Welfare Act of 1970 and the "Guide for the Care and Use of Laboratory Animals" prepared by the Institute of Laboratory Animal Resources - National Research Council.

This report has been reviewed by the Office of Public Affairs (PA) and is releasable to the National Technical Information Service (NTIS). At NTIS, it will be available to the general public, including foreign nations.

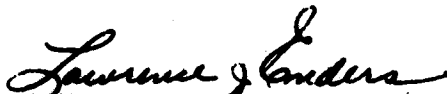
This technical report has been reviewed and is approved for publication.



DWAINE M. THOMAS, Ph.D.
Project Scientist



WILLIAM D. GIBBONS, Lt Col, USAF
Supervisor



LAWRENCE J. ENDERS
Colonel, USAF, MC
Commander

UNCLASSIFIED

SECURITY CLASSIFICATION OF THIS PAGE (When Data Entered)

REPORT DOCUMENTATION PAGE		READ INSTRUCTIONS BEFORE COMPLETING FORM	
1. REPORT NUMBER 14 SAM-TR-79-40	2. GOVT ACCESSION NO. AD-A087 100	3. RECIPIENT'S CATALOG NUMBER	
4. TITLE (and Subtitle) 6 LASER RAMAN SPECTROSCOPY OF ULTRAVIOLET-INDUCED CATARACTS IN RABBITS AND MONKEYS.		5. TYPE OF REPORT & PERIOD COVERED 9 Final Report Sep 77 - Feb 79	
7. AUTHOR(s) 10 Dwayne M. Thomas, Ph.D. Kenneth L. Schepler, Captain, USAF		8. CONTRACT OR GRANT NUMBER(s)	
9. PERFORMING ORGANIZATION NAME AND ADDRESS USAF School of Aerospace Medicine (RZL) Aerospace Medical Division (AFSC) Brooks Air Force Base, Texas 78235		10. PROGRAM ELEMENT, PROJECT, TASK AREA & WORK UNIT NUMBERS 62202F 7757-02-53 17 22	
11. CONTROLLING OFFICE NAME AND ADDRESS USAF School of Aerospace Medicine (RZL) Aerospace Medical Division (AFSC) Brooks Air Force Base, Texas 78235		12. REPORT DATE 11 December 1979	
14. MONITORING AGENCY NAME & ADDRESS (if different from Controlling Office) 12 56		13. NUMBER OF PAGES 53	
		15. SECURITY CLASS. (of this report) Unclassified	
		15a. DECLASSIFICATION/DOWNGRADING SCHEDULE	
16. DISTRIBUTION STATEMENT (of this Report) Approved for public release; distribution unlimited.			
17. DISTRIBUTION STATEMENT (of the abstract entered in Block 20, if different from Report)			
18. SUPPLEMENTARY NOTES			
19. KEY WORDS (Continue on reverse side if necessary and identify by block number) Biological Opacities in laser-exposed eyes Cataract Rabbit lens Laser exposures of animals Raman spectra Lens Ultraviolet-induced cataracts Monkey lens <i>beta</i>			
20. ABSTRACT (Continue on reverse side if necessary and identify by block number) The Raman spectra of normal rabbit and monkey lenses have been recorded over the range of 0-4000 cm^{-1} . Spectral results indicate that protein conformation is predominantly β -pleated sheet. Polarization measurements and assignments for most of the bands have been made; the spectral region for water indicates extensive hydrogen bonding. A nitrogen laser, operating at 337 nm, was used to produce cataracts in rabbit and monkey lenses; the Raman spectra of the cataractous lenses were also recorded. Spectral changes, observable in the water region, are correlated with a mechanism of ultraviolet cataractogenesis.			

DD FORM 1473 EDITION OF 1 NOV 65 IS OBSOLETE

UNCLASSIFIED

SECURITY CLASSIFICATION OF THIS PAGE (When Data Entered)

14007 cm 317000

CONTENTS

	<u>Page No.</u>
INTRODUCTION	5
MATERIALS AND METHODS	5
Laser Exposure Systems	5
Anesthesia Techniques	5
Animal Exposures	6
Raman Spectroscopy	7
Amino Acids and Other Lens Components	9
RESULTS AND DISCUSSION	9
Exposure Effects on Animal Eyes	9
Raman Spectroscopy of Rabbit Lenses	9
Raman Spectroscopy of Monkey Lenses	19
Amino Acids	24
Subthreshold Experiments	24
REVIEW OF RESEARCH	25
ACKNOWLEDGMENTS	25
REFERENCES	26
APPENDIX A: RAMAN SPECTRA OF BIOLOGICALLY IMPORTANT MOLECULES IN THE RABBIT AND MONKEY LENSES, AS RELATED TO RADIATION EFFECTS (Figs. A-1 to A-8)	29
APPENDIX B: RAMAN SPECTRA OF AMINO ACIDS IN RABBIT AND MONKEY LENSES (Figs. B-1 to B-33).	35

Illustrations

(Text)

<u>Fig. No.</u>		<u>Page No.</u>
1.	Setup for nitrogen laser exposure	7
2.	Raman sampling cell with rabbit lens in place	8
3.	Polarized Raman spectrum of balanced sterile saline	11
4.	Polarized Raman spectra of a normal rabbit lens	12
5.	Polarized high-gain Raman spectra of a normal rabbit lens	13
6.	Polarized Raman spectra of a UV laser-induced cataract in a rabbit lens	14
7.	Polarized high-gain Raman spectra of a UV laser-induced cataract in a rabbit lens	15
8.	Polarized low-gain Raman spectra of a normal monkey lens	20
9.	Polarized high-gain Raman spectra of a normal monkey lens	21

CONTENTS (Cont'd.)

Illustrations

(Text)

<u>Fig.</u> <u>No.</u>		<u>Page</u> <u>No.</u>
10.	Polarized low-gain Raman spectra of a UV laser-induced cataract in a monkey lens	22
11.	Polarized high-gain Raman spectra of a UV laser-induced cataract in a monkey lens	23

Table No.

1.	Observed frequencies, relative intensities, and assignments for the normal and cataractous rabbit lens	16
----	--	----

(Appendix A)

Fig. No.

A-1.	Cysteine-HCl (LG), 25 Sep 78	31
A-2.	Cysteine-HCl (HG), 25 Sep 78	31
A-3.	Glutathione - Reduced (LG), 2 Oct 78	32
A-4.	Glutathione - Reduced (HG), 2 Oct 78	32
A-5.	Glutathione - Oxidized (LG), 2 Oct 78	33
A-6.	Glutathione - Oxidized (HG), 2 Oct 78	33
A-7.	DL-Kynurenine, 25 Sep 78	34
A-8.	Tryptophan, 28 Aug 78	34

(Appendix B)

B-1.	Alanine (LG), 12 Apr 78	37
B-2.	Alanine (HG), 12 Apr 78	37
B-3.	Arginine (LG), 5 May 78	38
B-4.	Arginine (HG), 5 May 78	38
B-5.	Aspartic Acid (LG), 1 May 78	39
B-6.	Aspartic Acid (HG), 1 May 78	39
B-7.	Cystine (LG), 26 Apr 78	40
B-8.	Cystine (HG), 26 Apr 78	40
B-9.	Glutamic Acid (LG), 1 May 78	41
B-10.	Glutamic Acid (HG), 1 May 78	41
B-11.	Glycine (LG), 8 May 78	42
B-12.	Glycine (HG), 8 May 78	42
B-13.	Histidine, 28 Apr 78	43
B-14.	Isoleucine (LG), 21 Apr 78	44
B-15.	Isoleucine (HG), 21 Apr 78	44
B-16.	Leucine (LG), 19 Apr 78	45
B-17.	Leucine (HG), 19 Apr 78	45
B-18.	Lysine (LG), 3 May 78	46

CONTENTS (Cont'd.)

<u>Fig.</u>	<u>Page</u>
<u>No.</u>	<u>No.</u>

(Appendix B)

B-19. Lysine (HG), 3 May 78	46
B-20. Methionine (LG), 24 Mar 78	47
B-21. Methionine (HG), 24 Mar 78	47
B-22. Phenylalanine (LG), 24 Mar 78	48
B-23. Phenylalanine (HG), 24 Mar 78	48
B-24. Proline (LG), 26 Apr 78	49
B-25. Proline (HG), 27 Apr 78	49
B-26. Serine (LG), 20 Apr 78	50
B-27. Serine (HG), 20 Apr 78	50
B-28. Threonine (LG), 26 Apr 78	51
B-29. Threonine (HG), 26 Apr 78	51
B-30. Tyrosine (LG), 11 Apr 78	52
B-31. Tyrosine (HG), 11 Apr 78	52
B-32. Valine (LG), 2 May 78	53
B-33. Valine (HG), 2 May 78	53

Accession For	
NTIS GRA&I	<input checked="" type="checkbox"/>
DDC TAB	<input type="checkbox"/>
Unannounced Justification	
By _____	
Distribution/	
Availability Codes	
Dist	Avail and/or special
A	

LASER RAMAN SPECTROSCOPY OF ULTRAVIOLET-INDUCED CATARACTS IN RABBITS AND MONKEYS

INTRODUCTION

This research, on Raman spectroscopy of ultraviolet (UV)-induced cataracts in rabbits and monkeys, had four main objectives: (a) to develop a Raman technique for measuring spectra of rabbit and monkey lenses; (b) to measure Raman spectra before and after a UV laser exposure; (c) to determine molecules or groups responsible for any spectral differences; and (d) to formulate a mechanism of UV cataractogenesis identifying possible precursors to opacification. All of the objectives set forth in the protocol have been met. Considerable knowledge has been gained concerning UV laser exposures to rabbits and monkeys, surgical procedures of lens extraction, and lenticular spectral data (1-7). Also, from our work, new avenues of research have been opened toward characterizing other cataracts and clinical application of the Raman technique.

This effort used Raman spectroscopy as a nonperturbing molecular probe to quantify changes that have occurred during UV laser-induced cataractogenesis. Intact lenses enucleated from anesthetized rabbits and monkeys, previously exposed to various energies of UV laser radiation, were examined using Raman scattering; and changes in their Raman spectra after radiation exposure were noted. These changes were interpreted in terms of determining a damage mechanism.

MATERIALS AND METHODS

Laser Exposure Systems

Two different lasers were used for making ocular exposures to ultraviolet radiation. Initially, a Spectra Physics Model 185 helium-cadmium (HeCd) laser (1250 W. Middlefield Rd., Mt. View, Calif. 94042) was used; this laser emitted a gaussian beam with a $\frac{1}{e}$ diam. of 1.5 mm at 325 nm with an average power of 25 mW. MacKeen et al. (8) used the same laser in their animal exposures. The majority of the animals were exposed with a Molelectron Model UV-1000 nitrogen (N_2) laser (177 N. Wolfe Rd., Sunnyvale, Calif. 94086). This laser operates at 337 nm and emits 10 pulses/sec, each pulse being 10 ns in duration. Average power measured at the laser aperture was nominally 50 mW, corresponding to 5 mJ/pulse. A Scientech Model 36-0001 laser power meter (5649 Arapahoe, Boulder, Colo. 80303), used for all power measurements, is likewise described in this report.

Anesthesia Techniques

Mature Dutch-belted rabbits (2-4 kg) and rhesus monkeys (3-5 kg), with normal corneas and lenses, were used in these experiments. A Nikon slit lamp

was used to monitor and record corneal and lenticular conditions before and after exposure. Atropine (1%, Alcon) was instilled one day before exposure as a mydriatic and cycloplegic agent, and tropicamide (1%, Alcon) was administered one-half hour before exposure. For anesthesia during exposure, rabbits were given intramuscular injections of Rompun (xylazine, 1.1 mg/kg, Haver-Lockhart) and Vetalar (ketamine hydrochloride, 2.2 mg/kg, Parke-Davis). Restraint anesthesia for monkeys was ketamine hydrochloride (10 mg/kg). The initial deep anesthesia for monkeys was sodium pentobarbital (20 mg/kg), administered intravenously; deep anesthesia was maintained as needed during an experiment.

Animal Exposures

Only rabbits were exposed to the HeCd laser. The rabbits were anesthetized, placed in a holding box, and their corneal surfaces exposed to the direct unattenuated beam of 25 mW for 8 to 32 min. These exposures did not produce definite lenticular opacification when observed with a slit lamp, and are not discussed further. Exposures with the Molelectron N₂ laser were then attempted. Zuclich and Connolly (9) have shown that the N₂ laser produced immediate cataracts in monkeys.

A diagram of the optical train used for N₂ laser exposures of both rabbits and monkeys is shown in Figure 1. The laser aperture is 6 x 25 mm, and the laser radiation is best described as being emitted in a TEM₁₀ mode. A quartz lens with a 20-cm focal length was used to focus the beam to a minimum diameter on or near each animal's corneal surface. This technique provided maximum energy density in the lens, since beam size changed very little in the small distance between the corneal surface and the lens. Minimum beam size was approximately 1 x 3 mm. Average power was measured, at the beam waist, both before and after an exposure; variations in average power were less than 10%.

For exposures above the threshold of lenticular damage, the pellicle (shown in Fig. 1) was not used. A Gerbrands Model 300 digital timer and a Model G-1166 shutter were used to time the pulse train exposures (usually 9.9 sec, but sometimes as short as 1 sec). The unattenuated laser beam (5 mJ/pulse) was used to make suprathreshold exposures. In order to create large opacities on the exposed lenses, a device was built to sweep the laser beam across an animal's cornea during an exposure. A stepping motor was used to move the animal platform up or down at switch-selectable rates. After some initial experimentation, the stepping motor switch was set to sweep the laser beam over 1 - 2 mm during a 9.9-sec exposure.

The beam-sweep device was also useful when performing subthreshold exposures. First, a suprathreshold exposure of 1 - 2 sec was made at a site slightly above the optical axis of the lens, while moving the animal less than 0.2 mm. Next, a subthreshold exposure was given for 9.9 sec, with simultaneous movement of the animal at approximately 0.01 - 0.02 cm/sec. Finally, another suprathreshold exposure was made at the site where the animal mover had stopped for the subthreshold exposure. The two suprathreshold exposures were later used as visible markers to show where the subthreshold exposure had taken place.

During a subthreshold exposure a pellicle was used to split approximately 5% of the beam into a Spectra Physics Model 403 PIN diode detector. The PIN diode signal was then displayed on a Hewlett-Packard Model 184A storage oscilloscope (1501 Page Mill Rd., Palo Alto, Calif. 94304). An entire 10-sec pulse

train could then be displayed on the oscilloscope. As confirmed by a photograph of the oscilloscope trace, the laser had not misfired during the exposure and the pulses were of uniform intensity.

Two different methods were used to reduce the energy density on the animal lens for subthreshold exposures. Initially, the quartz lens was moved 2 or 4 cm relative to the corneal surface, thus increasing from 3 mm to 5 or 7 mm the horizontal dimension of the beam striking the corneal surface. The alternative and ultimately more successful approach was to use attenuation filters that left the beam the same size but transmitted only one-third of the initial energy.

The animals were examined with a slit lamp immediately postexposure, a few hours later, and immediately prior to sacrifice and removal of the lens. The animals were killed with a lethal dose of Barb-Euthol (Haver-Lockhart), and the eyes were enucleated. Successful removal of animal lenses was accomplished using lenticular surgical techniques with the help of a surgical microscope; care was taken to assure that no damage occurred.

Raman Spectroscopy

After removal, the lenses were frozen immediately and stored, or deposited directly into the Raman sample container. Once frozen, the lenses became white opaque masses but still maintained their original shape. The lenses deposited in the sample containers were covered with a solution of balanced sterile saline, BSS (Alcon). Distilled water and normal saline were tried first; however, intact lens integrity degraded more rapidly in these solutions. In the BSS solution the lenses would stay optically clear and colorless for at least

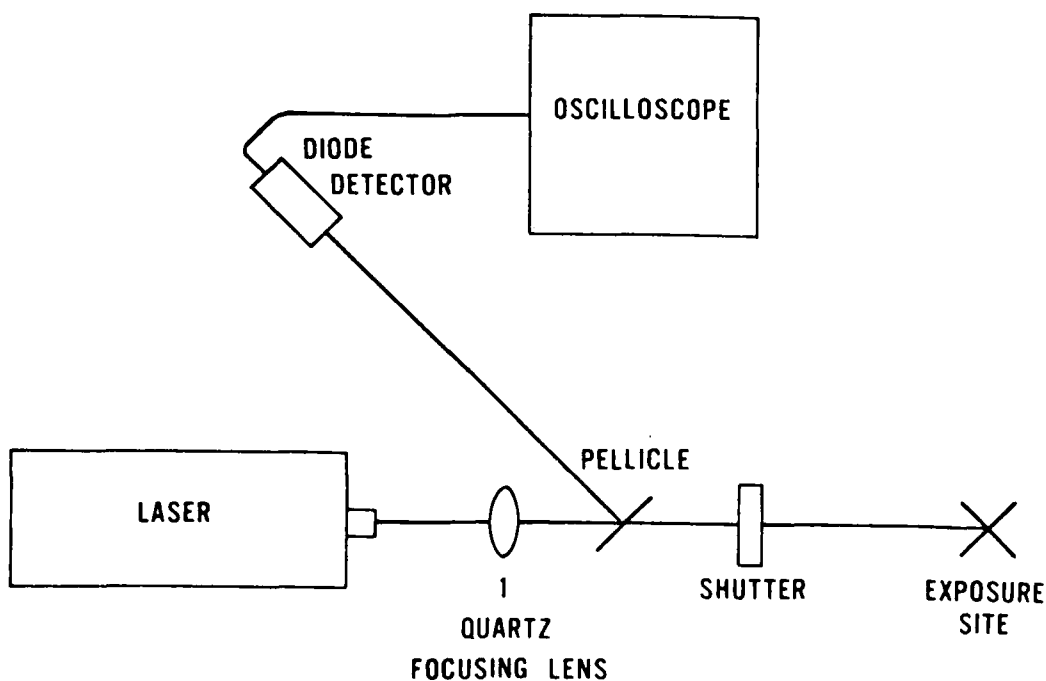


Figure 1. Setup for nitrogen laser exposure.
(Animal eye was positioned at exposure site.)

4 hr. After 4 hr, they began to turn cloudy in the capsular regions, spreading to the cortex after approximately 3 hr. The lens then appeared swollen due to water imbibition. Next, lens breakup commenced, with the epithelial layer separating first, followed by the cortex--leaving, undissolved, a solid nucleus. Frozen lenses were thawed in 0°C BSS, and allowed to reach room temperature slowly. A cylindrical quartz optical cell was used as a sample container; a lid for the cell was used throughout an experiment to help reduce evaporation of the BSS and prevent particulate from entering the cell. The lens was positioned with its posterior face on the cell bottom and approximately in the center.

Raman spectra were recorded using a Cary 82 spectrophotometer and a Spectra Physics 170-03 argon-ion laser; the principal wavelength was 514.5 nm. Other wavelengths were tried, but no significant differences in the spectral results were observed. A 90° scattering geometry was employed; an analyzer and a polarization scrambler were used for the polarized spectra. A scan time of 7 min was needed for the range 0-4000 cm^{-1} which gave spectral results of good resolution and reproducibility. The wavenumber accuracy from calibration results is approximately $\pm 2 \text{ cm}^{-1}$. Photon counting techniques were used for all recorded spectra.

The opti-cell is shown in Figure 2. The laser beam enters the bottom of the cell, passes through the lens and BSS, and exits through the top. The power of the transmitted beam passing through the cell lid is monitored throughout an experiment. For 3 - 4 hr of spectral recording, no appreciable change in relative laser beam power could be detected. This observation of constant transmitted beam power confirmed the absence of gross optical changes in lens integrity, while identical spectral results recorded at the beginning and end of an experiment indicated no significant subtle changes. Also shown in Figure 2 is the image that can be seen by the spectrometer. With this small image size,

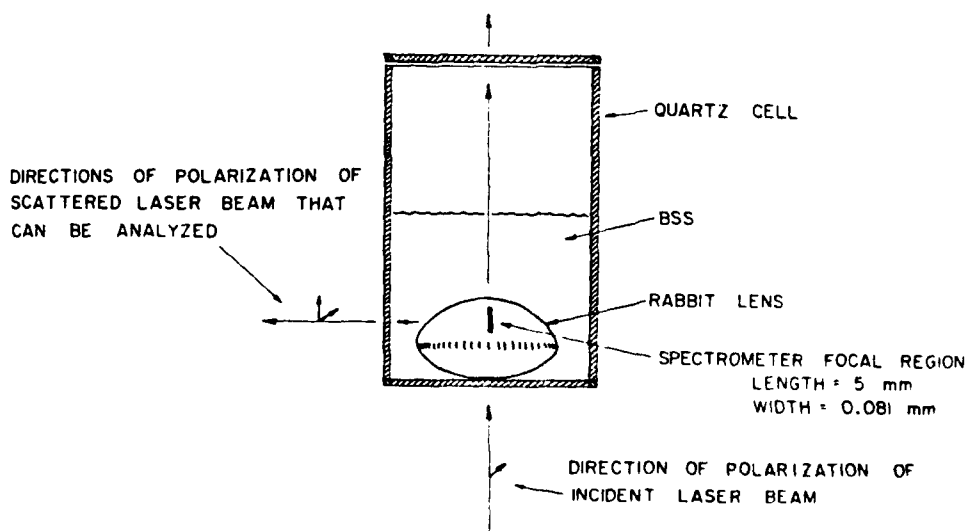


Figure 2. Raman sampling cell with rabbit lens in place.
[BSS = balanced sterile saline]

different regions of the lens can be examined easily. The laser beam can be positioned to pass through the image; at this point the region of interest can be located. Laser beam alignment is facilitated with the use of a Zeiss surgical microscope which provides magnification for visual manipulation. The laser beam power was varied from 100 mW to 2W at the sample for one experiment; no spectral or visible changes occurred for powers less than 1W hitting the sample. The actual experiments were recorded using laser powers of 100 - 300 mW at the sample. Thus, we assumed that the lens did not undergo any spectrally observable changes during lens extraction or Raman measurements.

Amino Acids and Other Lens Components

To help in spectral interpretations, the Raman spectra of known lens components were recorded. All biochemicals were obtained from Sigma Chemical Company and Calbiochem, and were used without further purification. Samples were powders, and Raman spectra were recorded in the Cary Solid Sample Holder for 90° scattering. Some samples were very sensitive to the 514.5 nm laser light, and readily decomposed upon irradiation; for these samples, the condensing lens was removed, thereby reducing the energy density incident on the material. For the respective amino acids a low-gain survey scan was made, followed by a high-gain recording. These spectra are shown in Appendix A (Figs. A-1 to A-8) and Appendix B (Figs. B-1 to B-33).

RESULTS AND DISCUSSION

Exposure Effects on Animal Eyes

Exposures to the N₂ laser for durations as short as 1 sec (10 pulses) were found to produce visible lenticular opacities in rabbits. These opacities were not immediately observable, but became apparent several hours later. The opacities reached maximum density in 1 - 2 days, with no change thereafter. For monkeys, some exposures produced immediately observable opacities; and, in all cases, the monkey lens opacities developed at a faster rate. Considerable corneal clouding and epithelial obliteration were present immediately after exposure of the eyes of rabbits and monkeys. However, the corneas healed completely within 1 - 2 days.

Raman Spectroscopy of Rabbit Lenses

The background spectrum of BSS for the range 0-4000 cm⁻¹ is shown in Figure 3. The only observable band systems are those from water; namely, at 1640, 3250, and 3400 cm⁻¹. At very high-gain levels, two very weak bands appeared at 927 and 1415 cm⁻¹, as a result of salts dissolved in the BSS. This gain level, however, is much higher than that used in the experiment, so these bands did not interfere. Since the rabbit lens does contain approximately 65% water, the water bands will appear in the spectrum. Polarization results indicate the 1640 cm⁻¹ band to be depolarized, and the 3250 and 3400 cm⁻¹ bands to be polarized. In fact, in the crossed polarized orientation (\perp) another component appears at 3450 cm⁻¹. The 3400 cm⁻¹ band is strongest in intensity, with the 3250 cm⁻¹ band as a shoulder. The polarized Raman spectra of a normal rabbit lens is shown in Figure 4. A high-gain recording for the spectral range 0-2000 cm⁻¹ is shown in Figure 5. The cataractous rabbit lens spectra are

shown in Figures 6 and 7 with the same designation as for the normal lens. The same lens was used for both normal and cataractous spectra; the laser beam and spectrometer image were moved within the lens to coincide with one of these areas. The frequencies, intensities, and assignments for the experimental results are listed in Table 1. Normal rabbit lens spectra were exactly reproducible from one rabbit to another. Several cataractous lenses were recorded, and all gave results similar to those in Figures 6 and 7.

Spectrally the lens is composed of protein and water (10, 11). Water can be of two types: intracellular and extracellular. The intracellular water can be bound to the proteins as water of crystallization or arranged in a layered structure. This intracellular environment for water is expected to alter slightly its vibrational characteristics as compared with those in the free state. The protein in the rabbit lens consists primarily of α , β , and γ crystallins. In the lens, there is also glutathione, tryptophan and, possibly, cysteine and/or cystine. Considerable structural investigations have been completed on these proteins. The amino acid composition is known; however, the sequences are still in question. The secondary structure is known, but the tertiary and quaternary structures are unknown. Raman spectra have been recorded for a number of crystallins, and assignments have been based on interpretation of model compounds. Protein conformations have been explained using these results. Principally, the position of the amide I vibration (a C=O stretch) and the amide III vibration (a mixed N-H bend and C-N stretch) are the key indicators of conformation (12-15).

The spectral results observed here support previous Raman work with bovine lenses, in which the amide I and III bands appeared at frequencies indicative of the anti-parallel β -pleated sheet conformation (16, 17). We observe bands at 1669 and 1235 cm^{-1} , and assign these bands to the amide I and amide III vibrations, respectively. Thus, the position of these bands indicates that the crystallins in the rabbit lens assume primarily the β -pleated sheet conformation. Little can be said of the random coil or α -helix conformations; for these could be present in small amounts, and their corresponding bands could be concealed in the background. The remaining bands in the 0 - 2000 cm^{-1} region can be assigned to specific amino acid vibrations. A continuum from 0 to 400 cm^{-1} indicates no resolvable lattice mode structures. No S-S vibrations are indicated, but an S-H band is at 2575 cm^{-1} . This band could be due to the presence of glutathione or cysteine. In the free state, cysteine has an S-H band at 2560 cm^{-1} , while glutathione has an S-H band at 2530 cm^{-1} ; thus, a tendency exists to favor assigning the 2575 cm^{-1} band to cysteine. The most predominant bands in the 0 - 2000 cm^{-1} region come from phenylalanine, tyrosine, and tryptophan. The main band for phenylalanine is located at 1003 cm^{-1} , for tyrosine at 830 cm^{-1} , and for tryptophan at 759 cm^{-1} . The C-H and N-H stretching vibrations and water bands are in the region from 2800 to 4000 cm^{-1} . The water-band system is quite interesting. The two observed bands are at 3280 and 3400 cm^{-1} . In the free-water spectrum, the bands are at 3250 and 3400 cm^{-1} . The lower frequency component, 3250 cm^{-1} , corresponds to more highly hydrogen-bonded water; however, in going from the free state to a lenticular environment, this band shifts by 30 cm^{-1} to a higher frequency (less hydrogen-bonded). This band can conceivably be assigned to N-H vibrations; however, the observed N-H band intensities for different free amino acids appear to be too weak for the 3280 cm^{-1} band intensity.

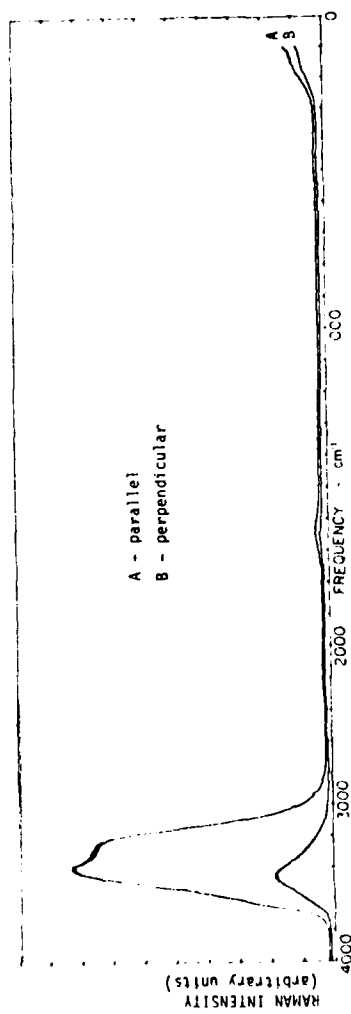


Figure 3. Polarized Raman spectrum of balanced sterile saline. [Instrument settings: laser = 514.5 nm, 430 mW at the sample; spectral bandwidth = 4 cm^{-1} ; gain = 100,000 counts/sec; pen period = 0.5 sec; and scan speed = $5 \text{ cm}^{-1}/\text{sec}$.]

[NOTE: In Figs. 3 - 7, (A) corresponds to light analyzed parallel to the incident beam polarization; (B) corresponds to the light analyzed perpendicular.]

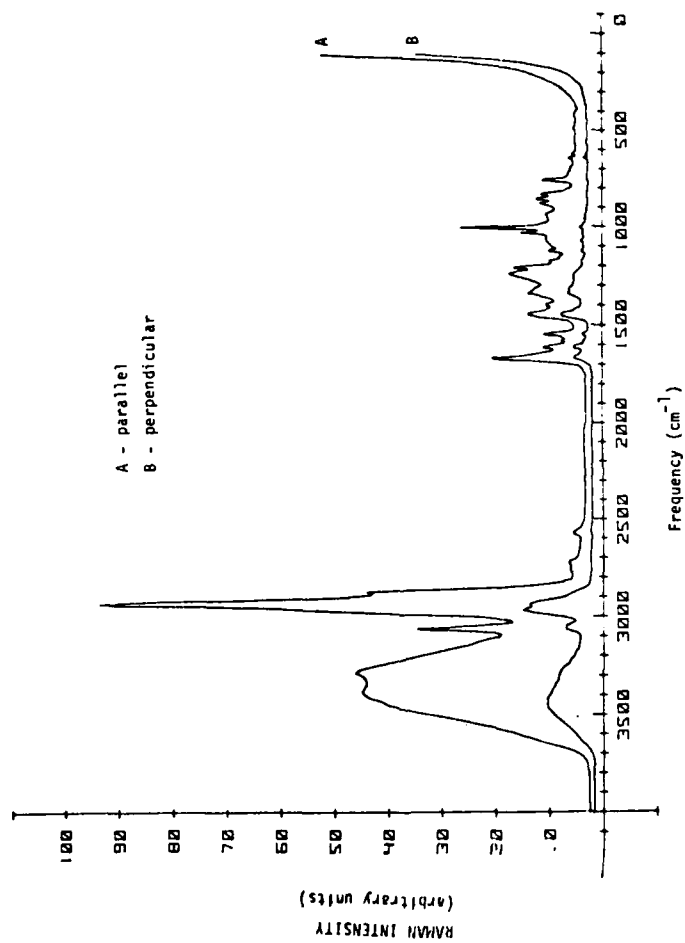


Figure 4. Polarized Raman spectra of a normal rabbit lens. [Instrument settings: laser = 514.5 nm, 235 mW at the sample; spectral bandwidth = 6 cm^{-1} ; gain = 90,000 counts/sec; pen period = 0.5 sec; and scan speed = 5 $\text{cm}^{-1}/\text{sec}$.]

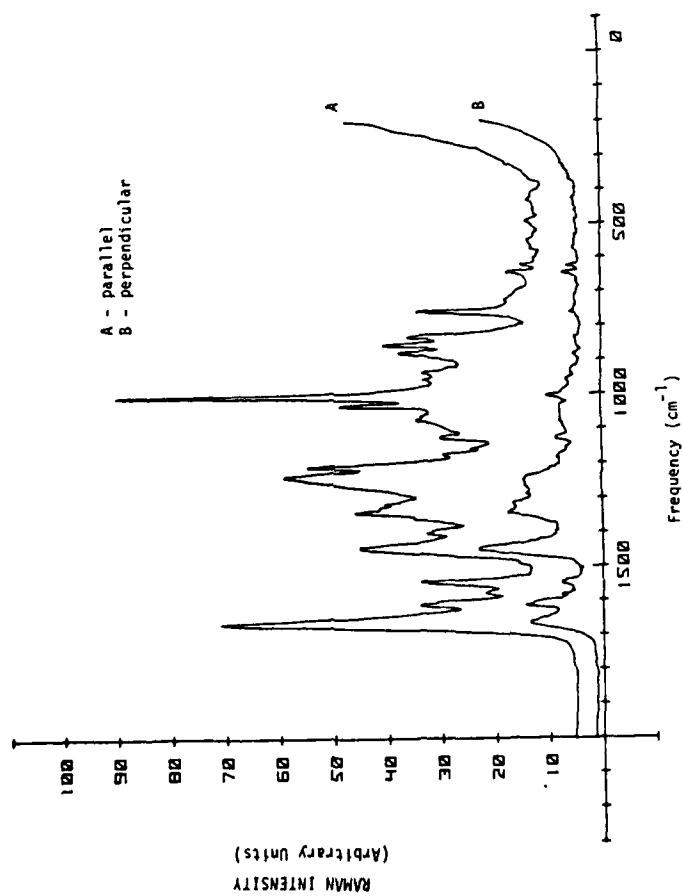


Figure 5. Polarized high-gain Raman spectra of a normal rabbit lens. [Instrument settings: laser = 514.5 nm, 235 mW at the sample; spectral bandwidth = 6 cm^{-1} ; gain = 20,000 counts/sec; pen period = 0.5 sec; and scan speed = 5 $\text{cm}^{-1}/\text{sec}$.]

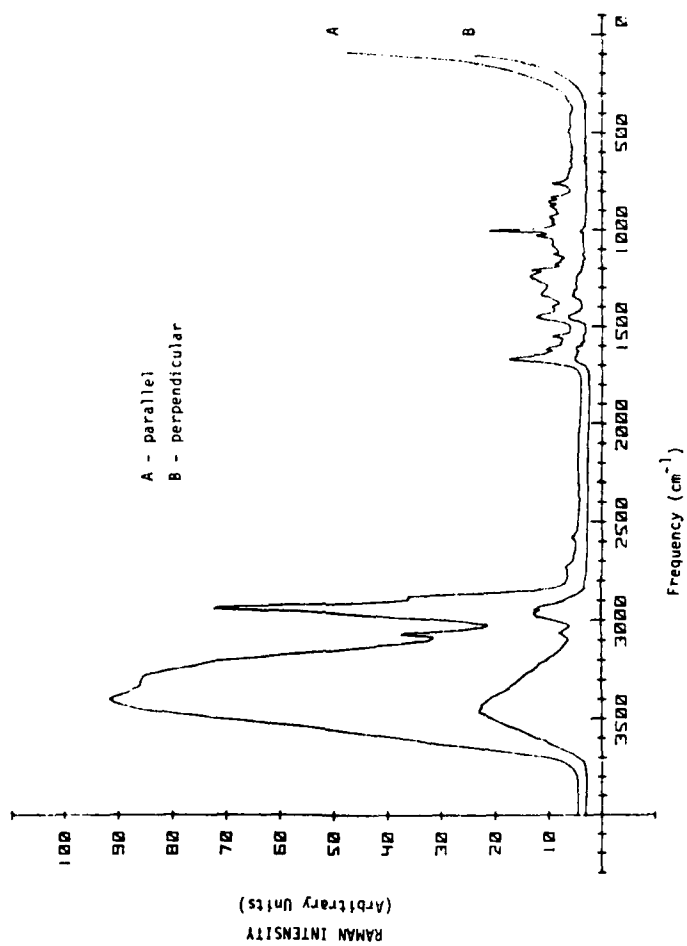


Figure 6. Polarized Raman spectra of a UV laser-induced cataract in a rabbit lens. [Instrument settings: laser = 514.5 nm, 235 mW at the sample; spectral bandwidth = 6 cm⁻¹; gain = 42,500 counts/sec; pen period = 0.5 sec; and scan speed = 5 cm⁻¹/sec.]

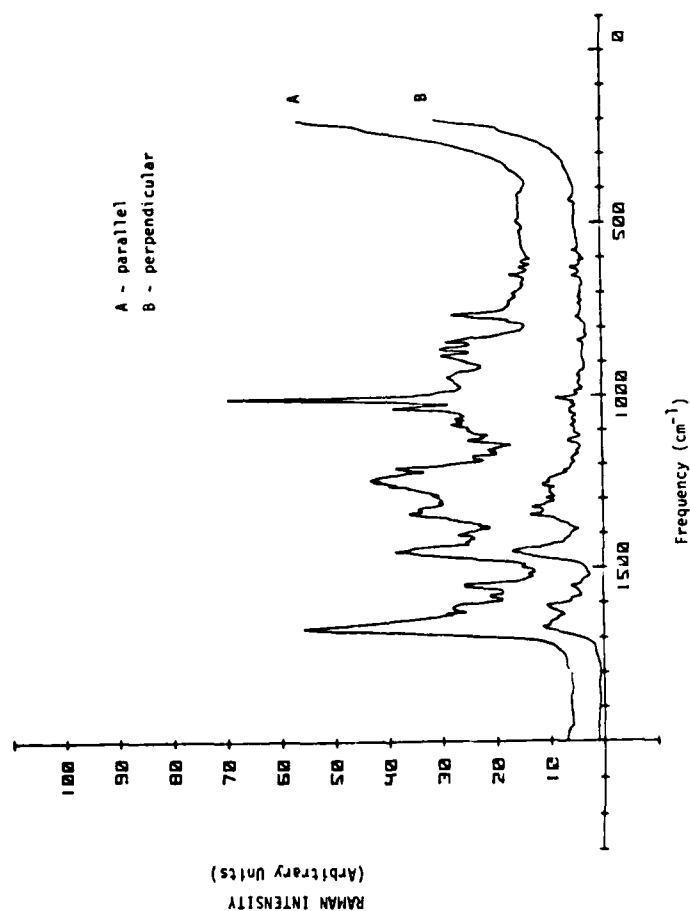


Figure 7. Polarized high-gain Raman spectra of a UV laser-induced cataract in a rabbit lens. [Instrument settings: laser = 514.5 nm, 235 mW at the sample; spectral bandwidth = 6 cm^{-1} ; gain = 9,500 counts/sec; pen period = 0.5 sec; and scan speed = 5 $\text{cm}^{-1}/\text{sec}$.]

TABLE 1. OBSERVED FREQUENCIES, RELATIVE INTENSITIES, AND ASSIGNMENTS FOR THE NORMAL AND CATARACTOUS RABBIT LENS

Frequency (cm ⁻¹) and Polarization	Normal	Relative intensity (arbitrary units)	Cataractous	Assignments
3450* p	8.3	low-gain (Fig. 4)	20.0	water
3400 p	41.0		87.0	water
3280 p	43.0		81.5	water
3060 p	31.1		33.2	C-H
3040* p	4.7		-	C-H
2970* p	13.0		10.5	C-H
2935 p	89.0		69.1	C-H
2870 p	40.2		32.0	C-H
2765 p	3.0		-	-
2720 p	3.0		2.7	-
2575 p	2.5		1.7	S-H
1669 p	65.2	high-gain (Fig. 5)	47.3	Amide I
1615 dp	28.4		21.7	Tyr
1603 dp	25.0		20.9	Phe
1583 p	15.4		14.3	Phe
1577 p	15.8		14.7	Trp
1548 p	27.7		19.0	Trp
1445 dp	36.5		-	CH ₂ def.
1400 p	25.1		19.0	-
1360 p	28.1		-	Trp
1340 p	38.5		27.9	Trp
1235 p	51.0		34.2	Amide III
1207 p	46.9		30.0	Phe
1174 p	21.7		15.0	Tyr
1157 p	16.5		11.8	C-N
1125 p	22.0		15.0	C-N
1070 p	25.7		18.0	C-N
1030 p	39.5		29.0	Phe
1003 p	81.2		58.9	Phe
958 p	23.6		17.6	C-C
935 p	24.0		19.0	C-C
870 p	27.0		19.0	Trp
855 p	31.0		19.3	Tyr
830 p	26.5		17.5	Tyr
759 p	24.0		15.6	Trp
644 dp	7.0		5.0	Tyr
620 dp	4.2		3.0	Phe
570 p	2.0		-	-
547 p	2.1		-	-
492 p	2.3		-	Cys-Cys?
420 p	1.2		-	-

*These bands appeared only in the perpendicular polarization.

[NOTE: Cys-Cys = cystine ; dp = depolarized; Phe = phenylalanine; Trp = tryptophan; and Tyr = tyrosine.]

The polarization results are also shown in Figures 4 - 7 and in Table 1. The lens, although in some respects resembling a uniaxial crystal, is really a gel-like material with a varying degree of order. To a good approximation, however, we can assume that an optic axis is still present; and enough ordering should exist to measure polarization parallel to and perpendicular to the optic axis. The optic axis is assumed to correspond to a line approximately connecting the anterior and posterior poles. Most of the bands in the spectra are polarized--including the amide I vibration at 1669 cm^{-1} , and the in-plane symmetric ring vibration for benzene in phenylalanine at 1003 cm^{-1} . The out-of-plane deformation for phenylalanine at 620 cm^{-1} is depolarized. In the perpendicular polarization spectra, three new bands appeared in the high-frequency region: at 3450 , 3040 , and 2970 cm^{-1} . The band at 3450 cm^{-1} is probably another component of the broad-water band. The fact that the amide I and amide III bands are polarized suggests some symmetric character to their vibrations. Thus, the lens, although not a true solid or liquid, does possess enough local and dynamic order to allow secondary structure polarization effects. If the lens was more of a solid (i.e., uniaxial crystal) than a liquid (gel), then orientational changes would affect polarization results.

The lens was positioned in three different orientations for spectral recording: the axial position, in which the incident laser beam passes parallel to the lens optic axis, and the scattered beam exits at the equator; the equatorial position in which the incident beam passes perpendicular to the optic axis; and the slanted position in which the incident beam is skewed to the optic axis.

Primarily because of ease of positioning, the axial position was used for the four spectra presented. The equatorial and slanted positions, recorded under essentially identical instrumental conditions, are not shown in this report. The spectral results for all three orientations indicate that the three spectra are essentially identical in frequency and intensity. The most important observation concerned the polarization results among the three spectra--all were the same. This finding seems to indicate that the polarization observed is due to a local symmetry rather than any long-range ordering. Of course, the polarization effects from primary structures, such as phenylalanine (1003 cm^{-1}), can be free-molecule polarization effects; i.e., this is a symmetric in-plane vibration and should be polarized--assuming a random orientation of benzene rings. On the other hand, in the case of preferred orientation, in-plane/out-of-plane effects should be present. These were not observed. The polarization independence of the secondary structure band at 1669 cm^{-1} , with changing orientation, suggests the possibility of no preferred orientation in the cell fiber and consequently in the lens; otherwise, the symmetry of the vibration is such that the vibration is totally symmetric in all orientations. A fourth polarized spectrum was recorded of the cortex which had been partially dehydrated. The overall appearance of the spectrum is the same as for the normal, except for the polarization effects, the water region, and the 830 cm^{-1} band. The water bands appear with much less intensity, reflecting lost water. The water remaining is most likely water of crystallization attached to the protein. The 830 cm^{-1} band of tyrosine has decreased in intensity, possibly reflecting some hindered movement of its ring. Also, all bands appear to be depolarized. Apparently, all symmetry existing prior to dehydration has been lost; yet, the amide I and III bands have not shifted, nor have the other bands. The results of these orientation and dehydration spectra suggest the independence of molecular orientation within the fiber cell, and also the importance of

the protein water system at maintaining normal polarization effects and possible transparency.

The polarized Raman spectra of the cataractous region of a rabbit lens are shown in Figures 6 and 7. This was the same lens as for the normal lens spectra, except that the beam was moved to the cataractous site. In the comparison of normal vs. cataractous spectra, little difference exists in the low-frequency region; however, in the water-stretching region, considerable change occurs in band intensity. The 3400 and 3280 bands have shown a substantial increase in intensity. This is the major change observable, but a very slight change is also worthy of note. The peak height intensities of the phenylalanine band (1003 cm^{-1}), the β -pleated sheet band (1669 cm^{-1}), and the tryptophan band (759 cm^{-1}) were compared between the normal and cataractous spectra. In comparison of the intensity ratios of the $1003\text{ vs. }1669\text{ cm}^{-1}$ bands, essentially no difference existed in the normal vs. cataractous spectral bands; however, the $1003\text{ vs. }759$ ratio increased in passing to the cataractous spectrum, thus implying an intensity decrease in the 759 cm^{-1} band and, consequently, a concentration decrease for tryptophan. This observation is reasonable, because tryptophan has a UV peak absorption at 280 nm, which is in the vicinity of the 337-nm laser line. The absorption is broad and overlaps the 337-nm region. Thus, some tryptophan could have photochemically reacted to produce a decomposition product (e.g., N-formylkynurenine). A similar change, although not as pronounced, is seen in the 830 cm^{-1} band of tyrosine. This change also can be explained on the basis of UV absorption. This pathway has been discussed by a number of workers who advocate a free radical theory to explain radiation damage to the lens (18-20). MacKeen et al. (8) have also implicated photochemical processes involved in cataractogenesis from results of rabbit exposures to a 325-nm HeCd laser, although they presented no concrete evidence to support their suggestion.

The most obvious spectral change was the increase in water concentration. Reasons for this increase in water, other than cataractogenesis, were ruled out after a careful analysis of the system. The damage route appears to involve a breakup of the protein-water system by the UV laser light. Before laser exposure, distribution of protein and water is fixed, as indicated in the normal lens spectra. After exposure, water migrates to the site (or microinclusion), as evidenced by the increase in water-band intensities. This migration and destruction of long-range protein-water order results in opacification at the insult site. Thus, the mechanism of laser UV-induced cataractogenesis may involve disruption of the extensive hydrogen bonding that helps to maintain the long-range regularity of the protein-water system. This disruption of protein layers could lead to microinclusions as water slowly migrates into the injury sites. With the long-range order destroyed, irregularity of the index of refraction in the injured area could give rise to the scattering characteristics of cataracts. No conformational changes in the proteins were detected, thus indicating too little energy or resistance or stabilization against the insult. This finding would apparently rule out aggregation effects, which should result in decreased intensity for the 1669 cm^{-1} band. The resultant opacity can be explained on the basis of absorption of UV light and release of thermal energy that is enough to disrupt the protein-water network. Usually, thermal mechanism is meant to imply thermal denaturation of proteins (that is, a heat effect destroying the normal protein conformation). Even though we do not observe protein changes, we still contend that the damage route suggests mainly thermal processes. An analogous observation and conclusion occur when an intact rabbit

lens is boiled in water, this being clearly a thermal damage process. The lens becomes a hard white mass, yet spectral results indicate no protein conformation changes. Another mechanism, labelled the "acoustic" or "nonlinear" type, appears when a very high energy density is coupled with rapid absorption; the effect appears immediately. We doubt that this mechanism is present in our case. Our energy is on the borderline for observing acoustic effects; in most cases, the opacities intensified over several days. An unequivocal assignment of mechanism type is presently premature and needs further clarification. Interestingly, the observation of areas of increased water concentration is very similar to that of a galactose cataract; i.e., the formation of water clefts or water vacuoles (11).

Raman Spectroscopy of Monkey Lenses

Monkey lenses were considerably smaller than rabbit lenses and had to be handled in a somewhat different fashion. A smaller cylindrical container was used to provide mechanical stability. The monkey lens was also a faint yellow due to inherent fluorescent compounds, whereas the rabbit lens was completely colorless. As a result the Raman background scatter was slightly higher for the monkey lens spectra. A third difference between the monkey and rabbit lenses was in the adherence of the zonules to the equator. In the monkey lens, these zonules were very difficult to separate, resulting in several punctured capsules. Careful surgery proved to be the only way to remove the lenses successfully.

The monkey lens spectra, as recorded in the axial position (Figs. 8 and 9), were almost identical to the rabbit spectra--the low-frequency protein region being almost superimposable. In particular, the bands at 1669 cm^{-1} and 1238 cm^{-1} confirm the presence of the anti-parallel β -pleated sheet structure for the proteins in the monkey lens. Most of the other bands have the same intensity distribution and frequency position as the rabbit lens spectra, except for two main differences: The first involves the S-S vibration at 492 cm^{-1} assigned to cystine in the rabbit lens. In the monkey lens spectra, this vibration appears to be slightly more intense. The difference could be due to different orientation effects or concentration effects in the two lenses. The second major difference is in the 620 and 644 cm^{-1} bands. In the monkey lens spectra, these bands appear to be slightly weaker; again this reflects either orientation or concentration effects. These two differences are slight, but are above the uncertainty introduced by comparing different spectra recorded at different laser power levels, spectral bandwidth, and gain levels. In the higher frequency region, little change occurs in the C-H stretching modes; but the water-band intensities have increased significantly for the normal monkey lens. The frequency components at 3400 and 3280 cm^{-1} have not changed in position, but both have increased relative to the C-H 2935 cm^{-1} stretching mode. This increase is probably a result of increased water concentration in the normal monkey lens as compared with that in a rabbit lens. Some orientational effect could also be contributing to this increase. Polarization results for both the rabbit and monkey are the same, as already described.

The Raman spectra for the cataractous region of the monkey lens are shown in Figures 10-11. The spectral difference between cataractous and noncataractous lens tissue is essentially the same as for the rabbit lens: an increase in the water band system intensities. This increase is the only major change in

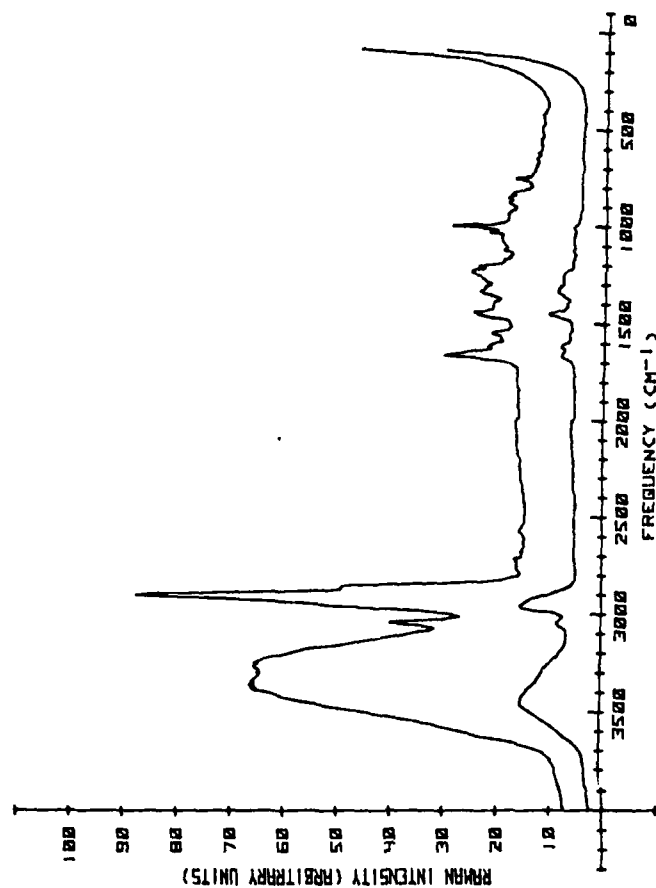


Figure 8. Polarized low-gain Raman spectra of a normal monkey lens. [Instrument settings: laser = 514.5 nm, 100 mW at the sample; spectral bandwidth = 8 cm⁻¹; gain = 75,000 counts/sec; pen period = 2 sec; and scan speed = 4 cm⁻¹/sec.]

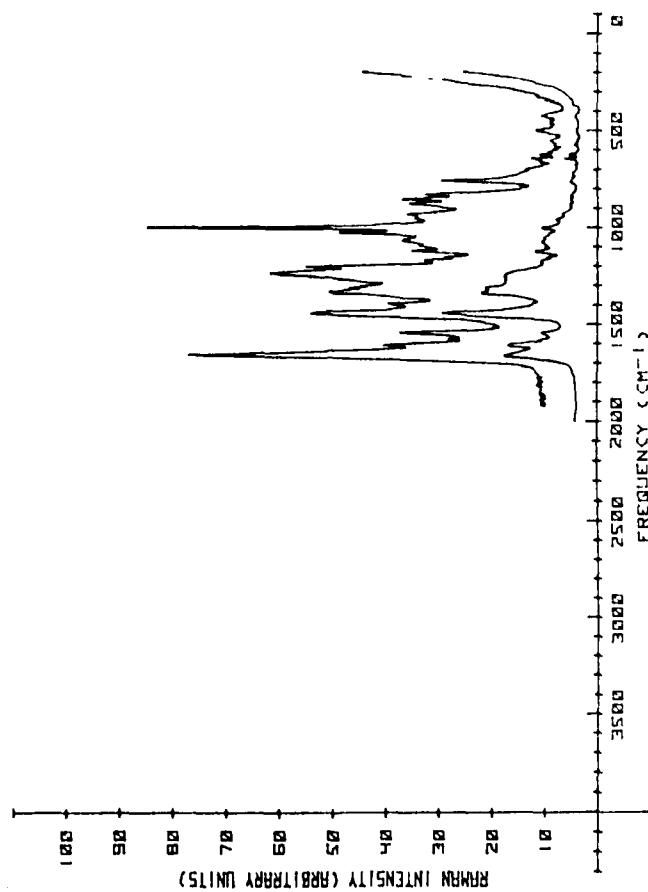


Figure 9. Polarized high-gain Raman spectra of a normal monkey lens. [Instrument settings: laser = 514.5 nm, 100 mW at the sample; spectral bandwidth = 8 cm^{-1} ; gain = 15,000 counts/sec; pen period = 0.5 sec; and scan speed = $1 \text{ cm}^{-1}/\text{sec}$.]

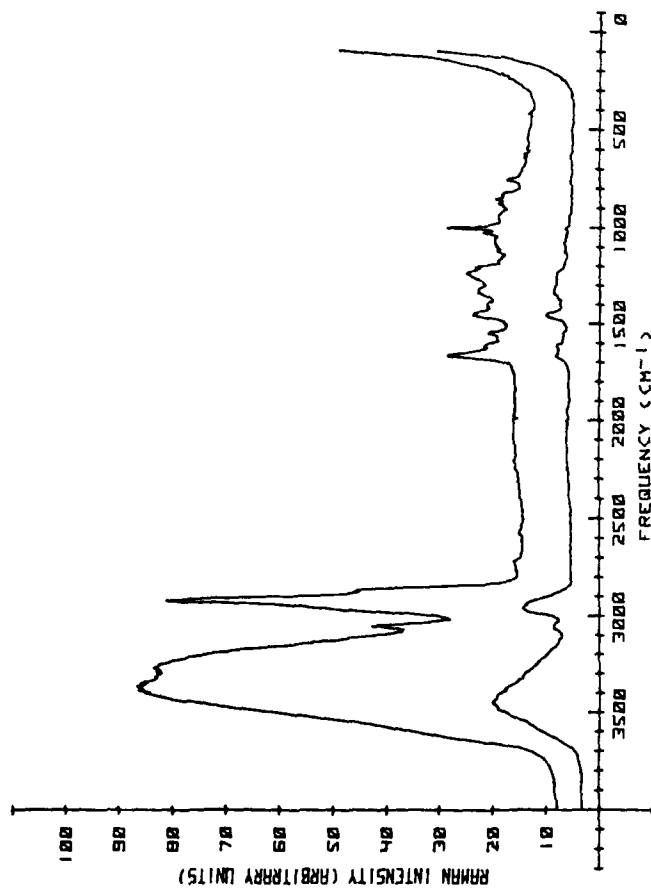


Figure 10. Polarized low-gain Raman spectra of a UV laser-induced cataract in a monkey lens.
 [Instrument setting: laser = 514.5 nm, 100 mW at the sample; spectral bandwidth = 8 cm⁻¹; gain = 45,000 counts/sec; pen period = 2 sec; and scan speed = 4 cm⁻¹/sec.]

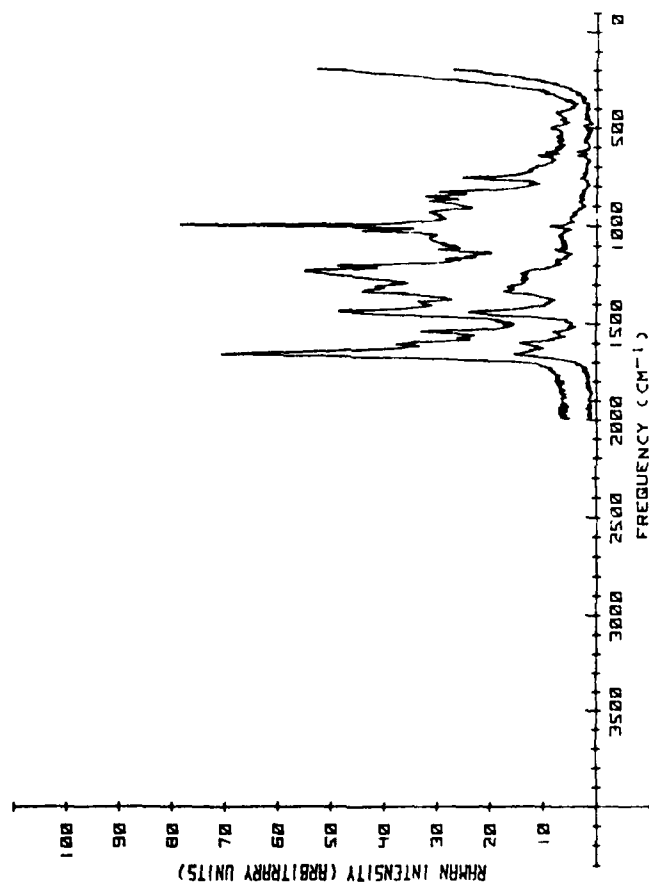


Figure 11. Polarized high-gain Raman spectra of a UV laser-induced cataract in a monkey lens.
[Instrument setting: laser = 514.5 nm, 100 mW at the sample; spectral bandwidth = 8 cm⁻¹; gain = 9,000 counts/sec; pen period = 5 sec; and scan speed = 1 cm⁻¹/sec.]

the spectra. Again, as with the rabbit lenses, a slight decrease is indicated in band intensities for tryptophan and tyrosine in the cataractous spectra. These results were expected, because the cataracts produced in both animals were very similar in appearance and in formation characteristics. The same damage mechanism appears to be in operation for the monkey and for the rabbit.

Amino Acids

A few chemicals in the lens were recorded, and the more important ones are shown in Appendix A. The three compounds--cysteine-HCl, glutathione-oxidized and reduced, and tryptophan--are present in the lens, but only tryptophan can be identified in the lenticular spectra. Kynurenine derivatives are thought to be formed from free radical reactions in the lens, and are thus important as an analytical measure of the amount of free radical formation; for free radical can induce further changes leading to cataracts. This particular compound gave no Raman spectrum, but did yield a fluorescence spectrum with a maximum at 570.2 nm, exciting at 514.5 nm.

The following 18 amino acids comprise the lenticular proteins in the lens of a normal rabbit:

alanine	histidine	proline
arginine	isoleucine	serine
aspartic acid	leucine	threonine
cysteine	lysine	tryptophan
glutamic acid	methionine	tyrosine
glycine	phenylalanine	valine

For these amino acids, the Raman spectra were recorded over the spectral range, 0-4000 cm^{-1} ; digitized; and replotted in an 8 x 10 in. format (Appendix B). Most of the vibrational band assignments have been made for these molecules. In the spectral region above 2000 cm^{-1} , especially around 3000 cm^{-1} , all of the molecules display a similar signature; this region contains C-H and N-H stretches. In the region below 2000 cm^{-1} , however, each molecule displays its individual features. Only a few of the modes of these molecules actually appear in the protein spectrum, and these modes have a distinct character to their vibration which elevates them above the protein backbone spectrum. These assignments have been discussed in connection with the rabbit and monkey lens experiments. Some of the amino acids were recorded as solid mixtures and as multicomponent solutions. Little correspondence existed between the solid mixtures, solution, and actual proteins in the lens. Some of the strong features do stand out, and this factor does aid in classifying a few of the bands in the lens spectra. A much better technique would be to record different concentrations of the α , β , and γ crystallins, and then to compare these data with the lenticular Raman spectra.

Subthreshold Experiments

Several subthreshold experiments were attempted in order to find spectral evidence of opacification before visual appearance, as indicated by slit-lamp examination. Marker lesions were used to define an exposure site; the subthreshold dose was located between the markers. Positioning the spectrometer laser beam between the markers was difficult and uncertain, leaving us in doubt of any results. In some of the exposed rabbits, the marker lesions after a month

appeared to have diffused across the subthreshold region. Also, with the marker lesion technique, it was difficult to quantify an exact energy distribution falling in the subthreshold area. In general these findings were inconclusive and will have to be examined more closely in the future.

REVIEW OF RESEARCH

We have reported the polarized Raman spectra of normal and UV laser-induced cataractous lenses in rabbits and monkeys. The lenticular proteins exist in the anti-parallel β -pleated sheet conformation; this does not change after the radiation insult and resultant cataract. The only major spectral change observed was the increase in intensity of the water-band system ($3280\text{--}3400\text{ cm}^{-1}$). This change is thought to correspond to the effect of the high power density and short pulse duration of the UV laser beam on the protein-water system. We believe that this ordered system is disrupted, leading to vacuolation at the sites of radiation insult. The results suggest that the major mechanism involved in suprathreshold laser UV cataractogenesis is thermal in nature--a heat-disruptive effect of the laser beam on the protein-water network, with no observable effects on protein conformation. Although photochemical or acoustic and/or nonlinear effects are not completely ruled out, they are certainly small as compared with thermal effects.

Some minor differences between monkey and rabbit lens spectra were noted, but these differences do not appear to affect the mechanism of cataractogenesis.

The experiments designed to produce cataracts in rabbits and monkeys have proved to be quite successful in revealing molecular level changes which have occurred after a UV-radiation insult. The mechanism proposed for UV-laser damage may be specific to the laser and not explain long-term or latent lenticular anomalies that may appear in certain other situations. For a comprehensive explanation, investigations of other types of cataracts would have to be undertaken and these results compared with ours for a unified damage mechanism. A unique Raman spectral signature has been obtained for UV laser-induced cataracts; the next logical step is to apply this technique to other radiation cataracts to determine differences or similarities between their spectra.

ACKNOWLEDGMENTS

We would like to thank Lieutenant Colonel George W. Mikesell, Jr., for his help in interpreting results from the slit-lamp examinations. For surgical help we wish to thank Lieutenant Colonel Stanley Hand, Jr., and Major Douglas J. Ivan. Technical assistance was provided by Senior Airman Kevin A. Toth and Technical Sergeant William D. Decker, and also by Mrs. Shirley F. Kane.

REFERENCES

1. Thomas, D. M., and K. L. Schepler. UV laser-induced cataracts. *Biophys J* 21(3): 189a (1978).
2. Schepler, K. L., and D. M. Thomas. Raman spectroscopy of intact primate lenses which have cataracts induced by ultraviolet radiation. *Biophys J* 25(2): 240a (1979).
3. Thomas, D. M., and K. L. Schepler. Raman spectra of UV-induced cataracts in rabbits and monkeys. *Gordon Res. Conf. (Lasers in medicine and biology)*, Meriden, N.H., 1978.
4. Thomas, D. M. The effects of temperature and orientation of an intact rabbit lens on the polarized Raman spectra. *Assoc. for Res. in Vision and Ophthalmol. (ARVO)*, Sarasota, FL, 1979.
5. Thomas, D. M., and K. L. Schepler. Raman spectra of normal and UV-induced cataractous rabbit lens. (To be published in: *Invest Ophthalmol Vis Sci*)
6. Schepler, K. L., and D. M. Thomas. Raman spectra of normal and UV-induced cataractous monkey lens. (Article in preparation)
7. Thomas, D. M. The effects of temperature and orientation of an intact rabbit lens on the polarized Raman spectra. (Article being reviewed)
8. MacKeen, D., S. Fine, and B. S. Fine. Production of cataracts in rabbits with the ultraviolet laser. *Ophthalm Res* 5:317 (1973).
9. Zuclich, J. A., and J. S. Connolly. Ocular damage induced by near-ultraviolet laser radiation. *Invest Ophthalmol* 15:760 (1976) [Now: *Invest Ophthalmol Vis Sci*]
10. Warwick, R. Eugene Wolff's anatomy of the eye and orbit. Philadelphia: W. B. Saunders, 1976.
11. Kuck, J. F. R., Jr. Chemical constituents of the lens, pp. 183-260. In C. N. Graymore (ed.). *Biochemistry of the eye*. New York: Academic Press, 1971.
12. Fanconi, B., and W. L. Peticolas. Simplified force field calculations of the low-frequency motions of the α -helix. *Biopolymers* 10:2223 (1971).
13. Miyazawa, T. Infrared spectra and helical conformations, pp. 69 - 101. In G. D. Fasman (ed.). *Poly- α -amino acids*. New York: Marcel Dekker, 1967.
14. Small, E. W., B. Fanconi, and W. L. Peticolas. Raman spectra and the phonon dispersion of polyglycine. *J Chem Phys (Lancaster)* 52:4369 (1970).
15. Yu, N. T., C. S. Lui, and D. C. O'Shea. Laser Raman spectroscopy and the conformation of insulin and proinsulin. *J Mol Biol* 70:117 (1972).
16. Yu, N. T., and E. J. East. Laser Raman spectroscopic studies of ocular lens and its isolated protein fractions. *J Biol Chem* 250:2196 (1975).

17. Schachar, R. A., and S. A. Solin. The microscopic protein structure of the lens with a theory for cataract formation as determined by Raman spectroscopy of intact bovine lenses. *Invest Ophthalmol* 14:380 (1975).
18. Borkman, R. F., and S. Lerman. Evidence for a free radical mechanism in aging and UV-irradiated ocular lenses. *Exp Eye Res* 25:303 (1977).
19. Kurzel, R. B., et al. Tryptophan excited states and cataracts in the human lens. *Nature* 241:132 (1973).
20. Weiter, J. J., and E. D. Finch. Paramagnetic species in cataractous human lenses. *Nature* 254:536 (1976).

APPENDIX A:

RAMAN SPECTRA OF BIOLOGICALLY IMPORTANT MOLECULES, IN THE RABBIT AND
MONKEY LENSES, AS RELATED TO RADIATION EFFECTS

[(LG) = low gain; (HG) = high gain]

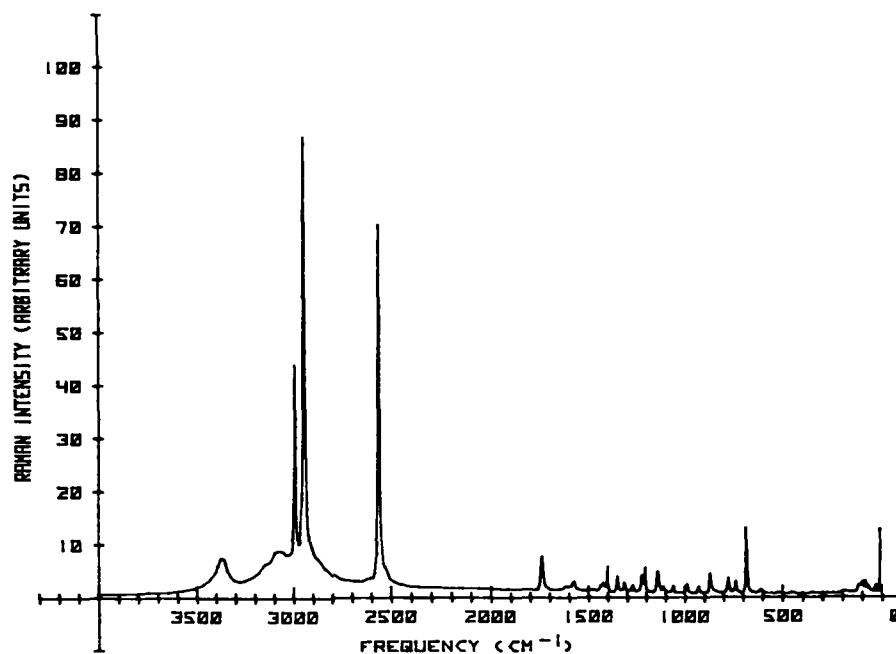


Figure A-1. Cysteine-HCl (LG), 25 Sep 78.

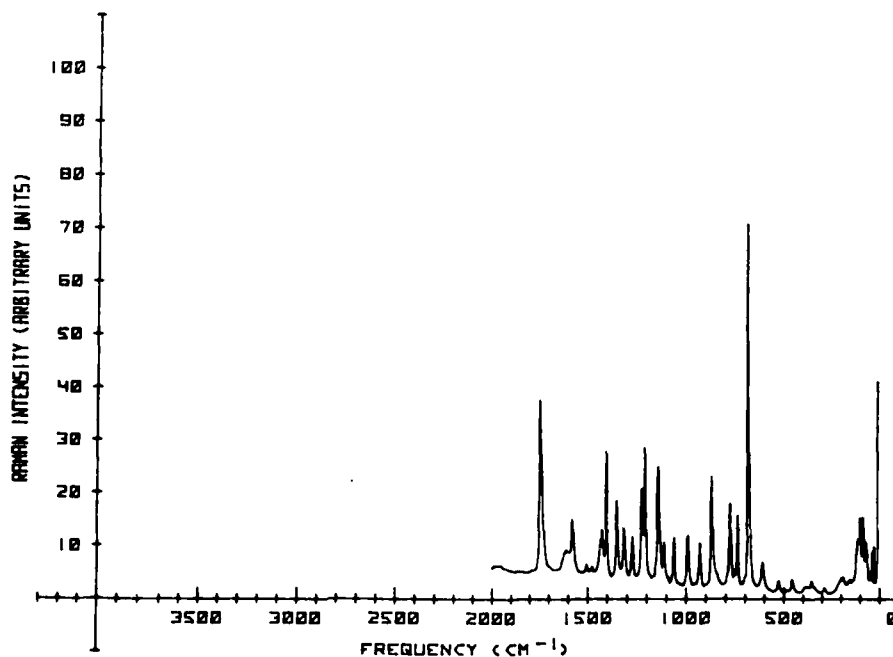


Figure A-2. Cysteine-HCl (HG), 25 Sep 78.

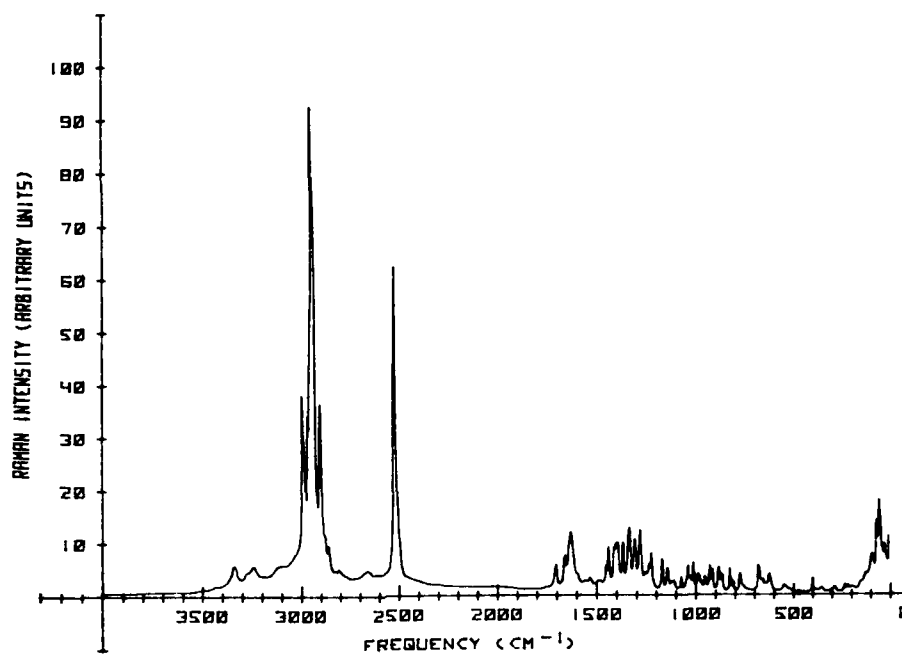


Figure A-3. Glutathione - Reduced (LG), 2 Oct 78.

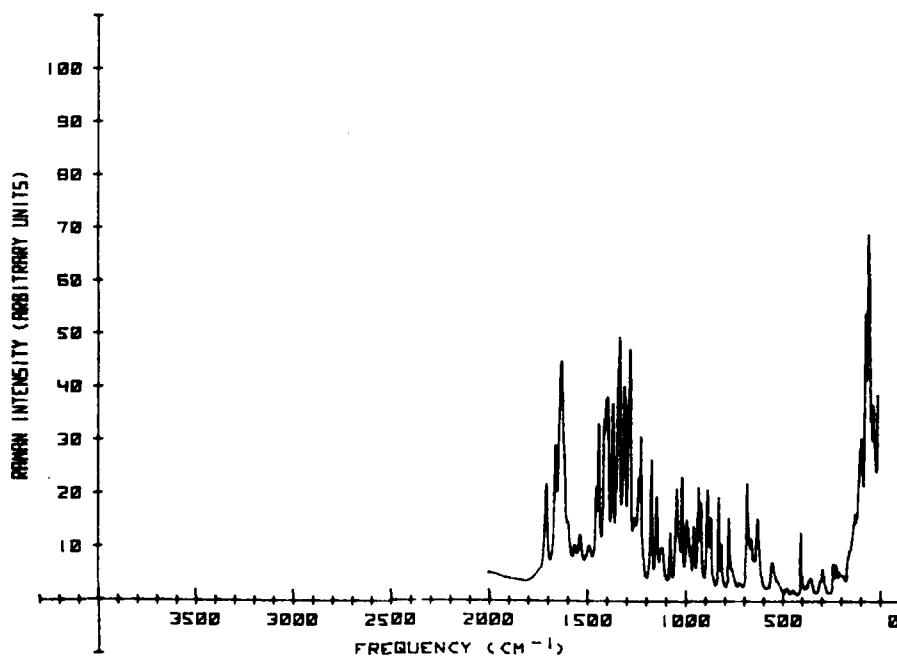


Figure A-4. Glutathione - Reduced (HG), 2 Oct 78.

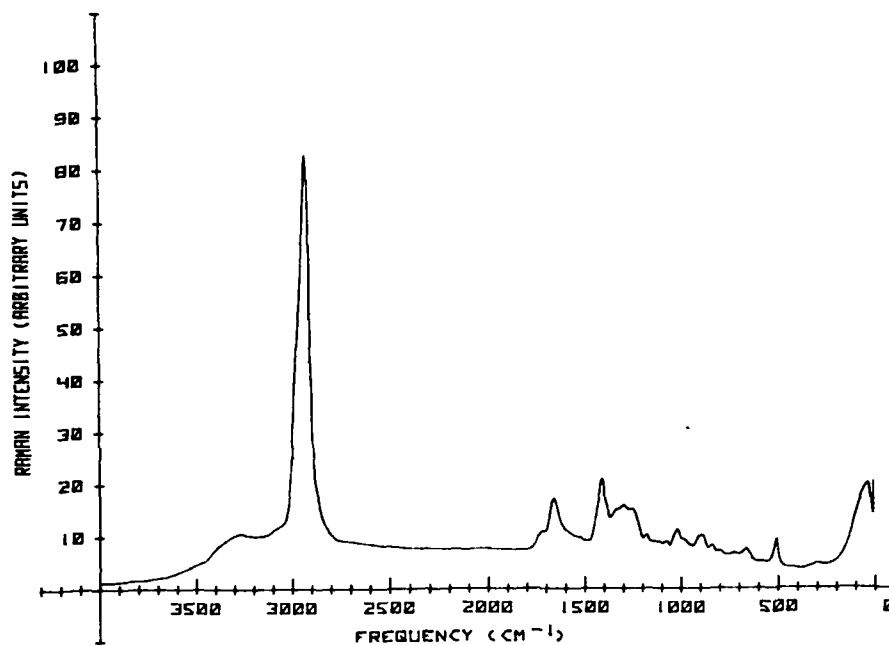


Figure A-5. Glutathione - Oxidized (LG), 2 Oct 78.

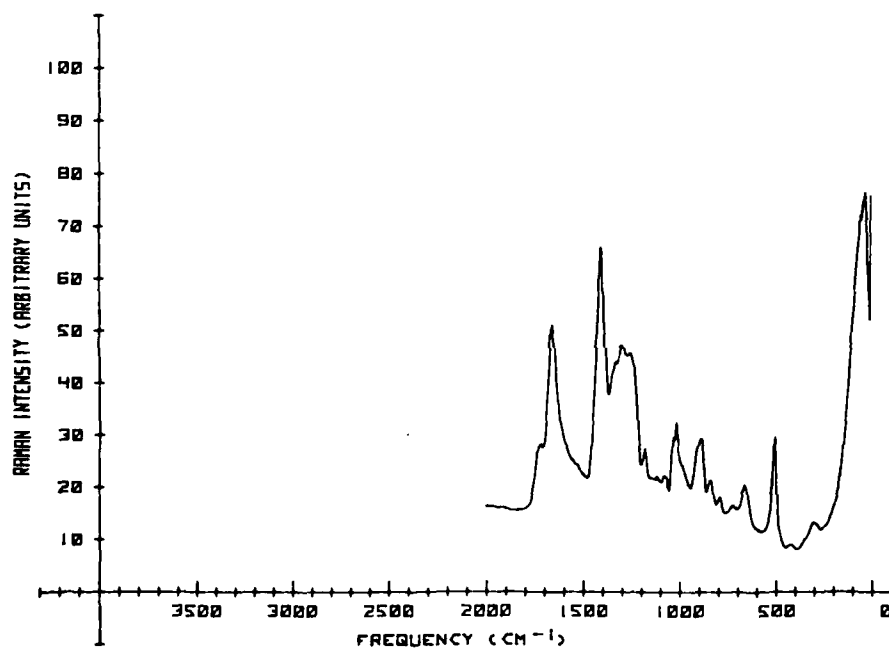


Figure A-6. Glutathione - Oxidized (HG), 2 Oct 78.

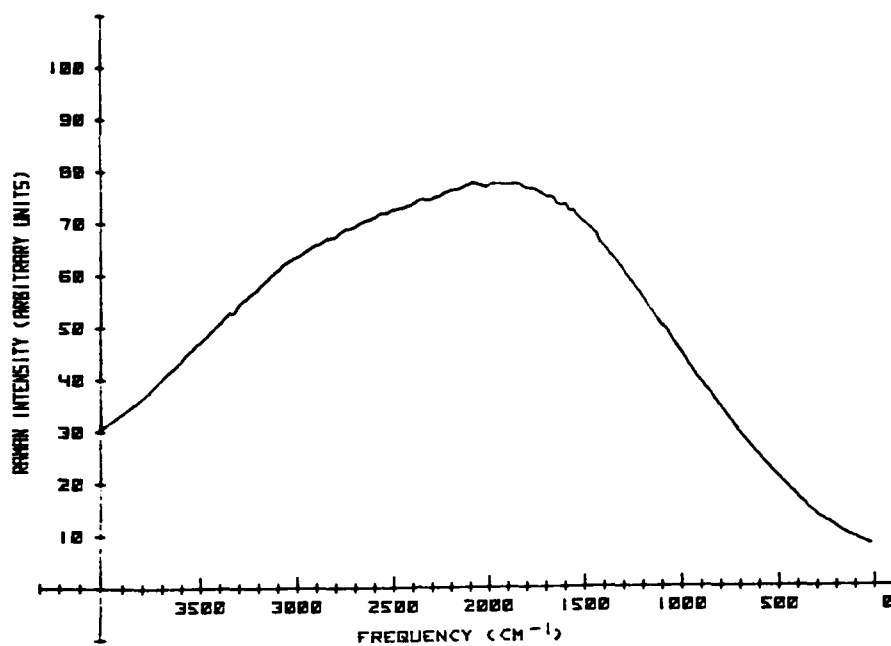


Figure A-7. DL-Kynurenine, 25 Sep 78.

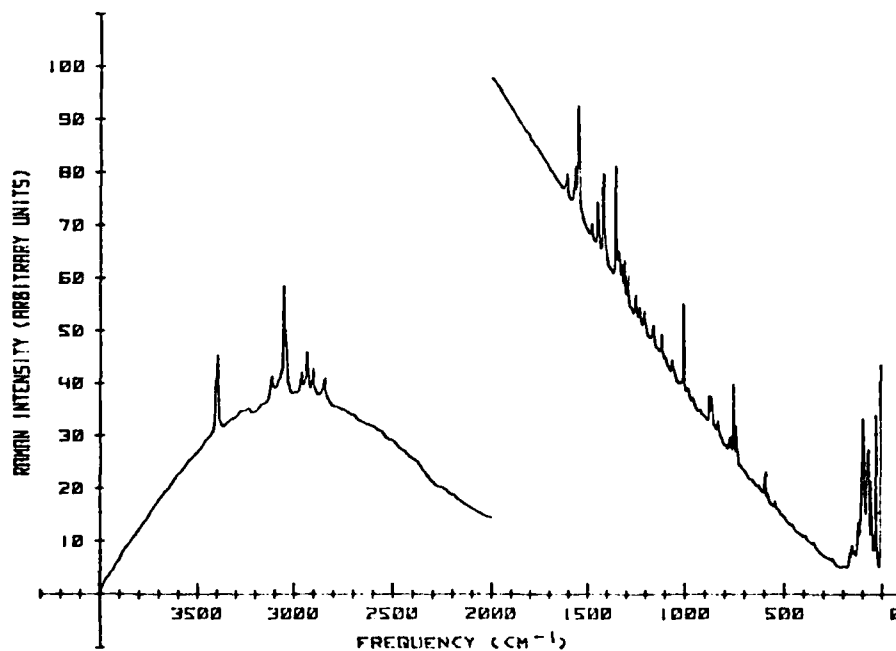


Figure A-8. Tryptophan, 28 Aug 78.

APPENDIX B:

RAMAN SPECTRA OF AMINO ACIDS IN RABBIT AND MONKEY LENSES

[(LG) = low gain; (HG) = high gain]

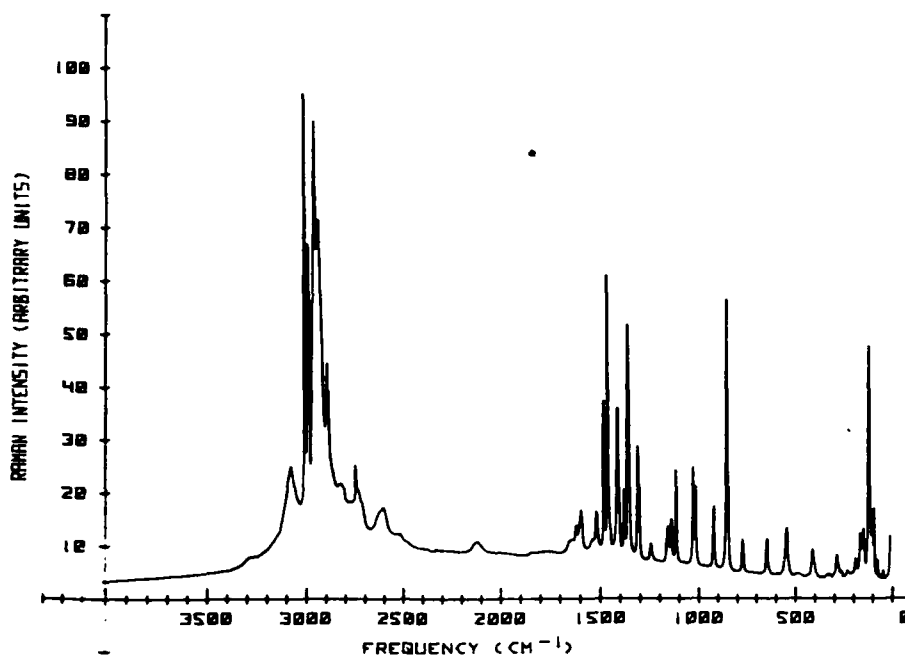


Figure B-1. Alanine (LG), 12 Apr 78.

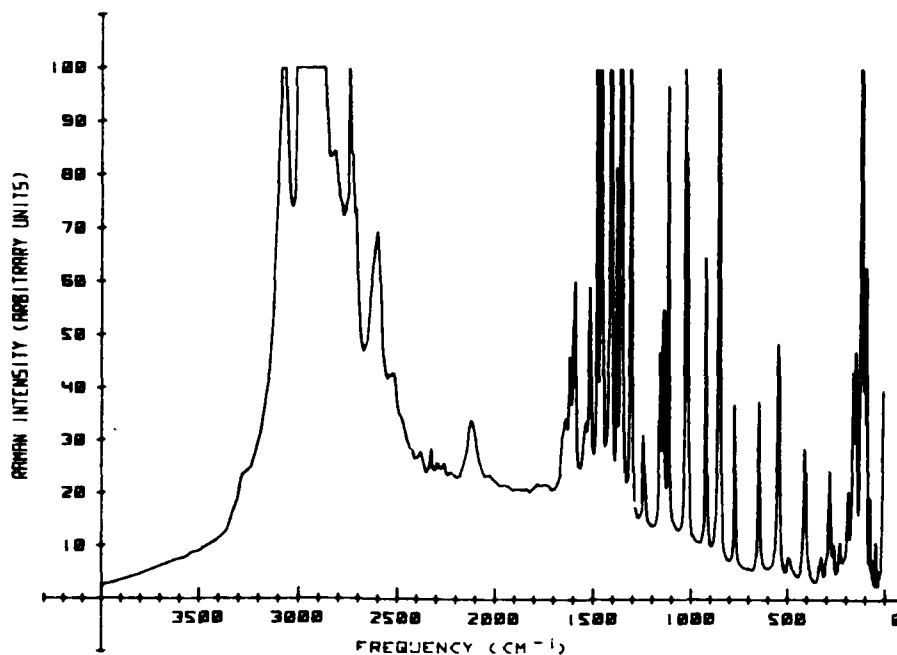


Figure B-2. Alanine (HG), 12 Apr 78.

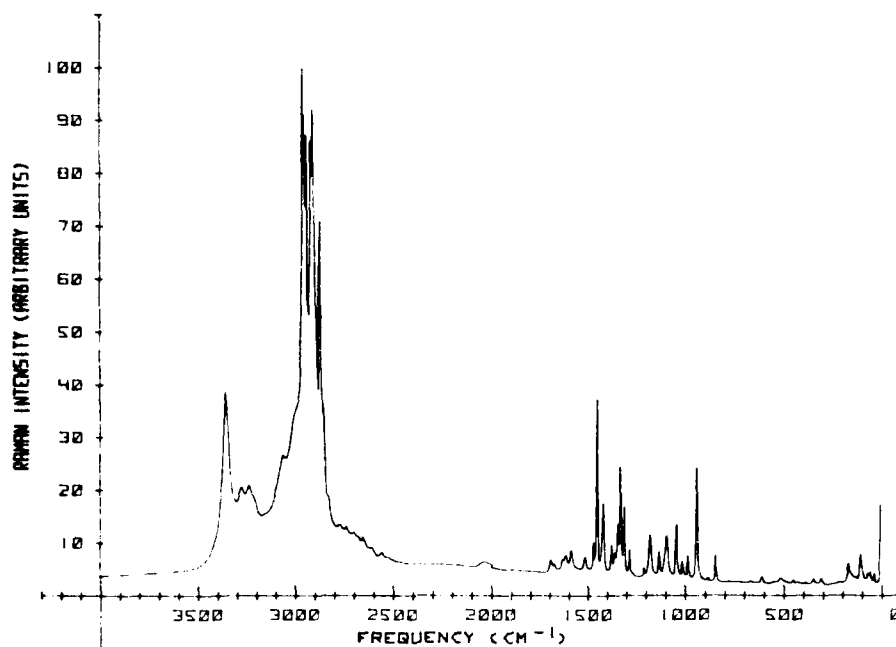


Figure B-3. Arginine (LG), 5 May 78.

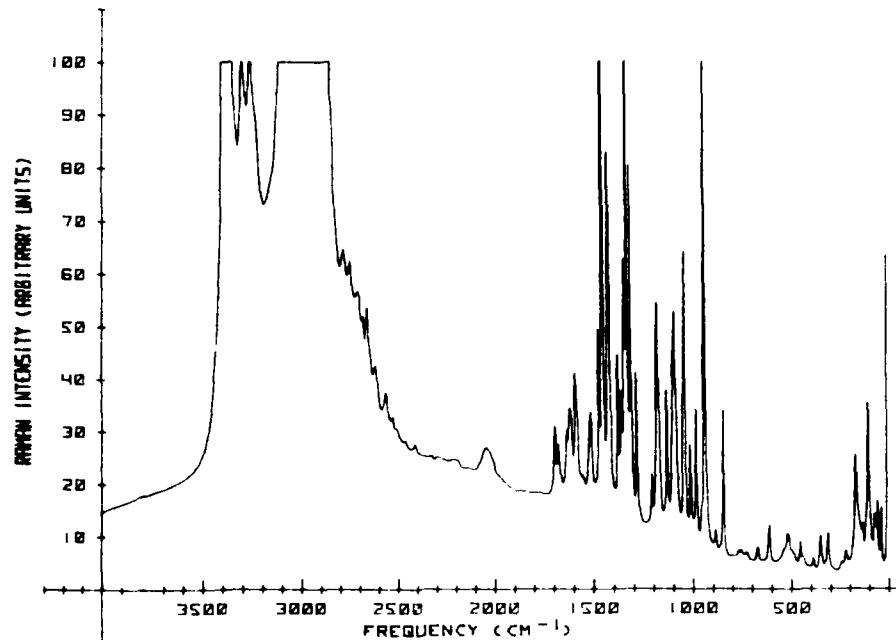


Figure B-4. Arginine (HG), 5 May 78.

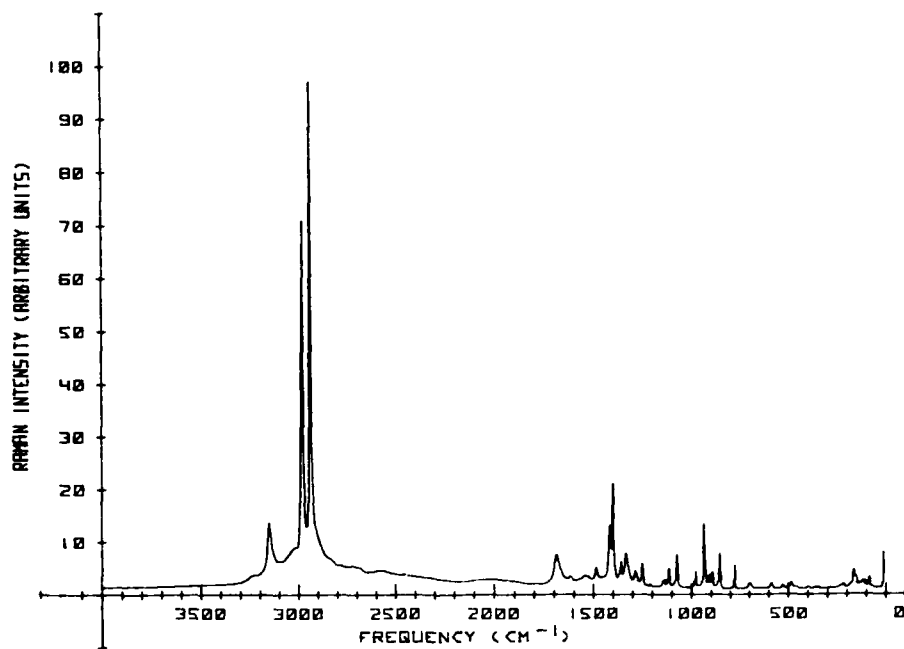


Figure B-5. Aspartic Acid (LG), 1 May 78.

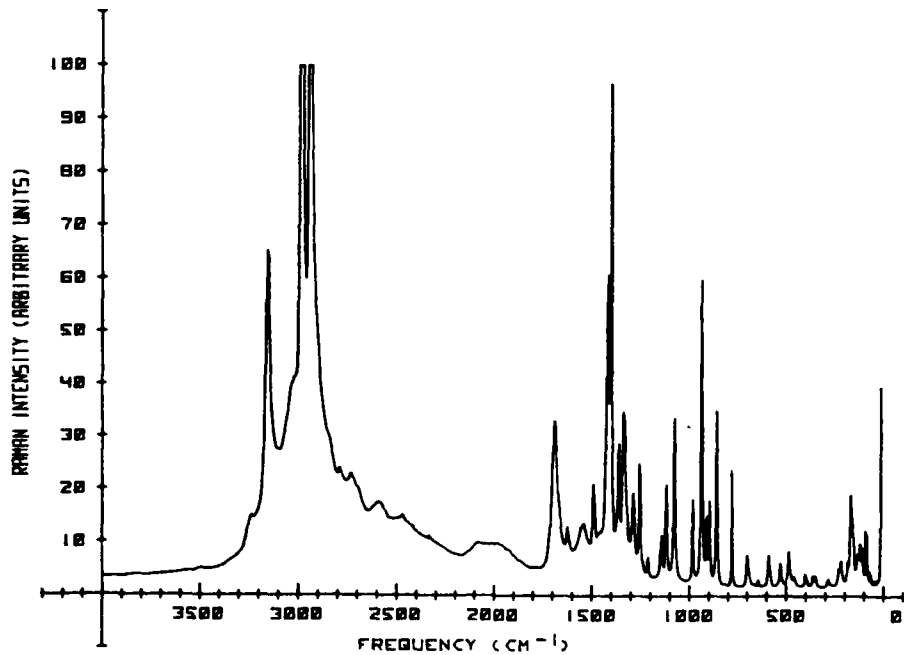


Figure B-6. Aspartic Acid (HG), 1 May 78.

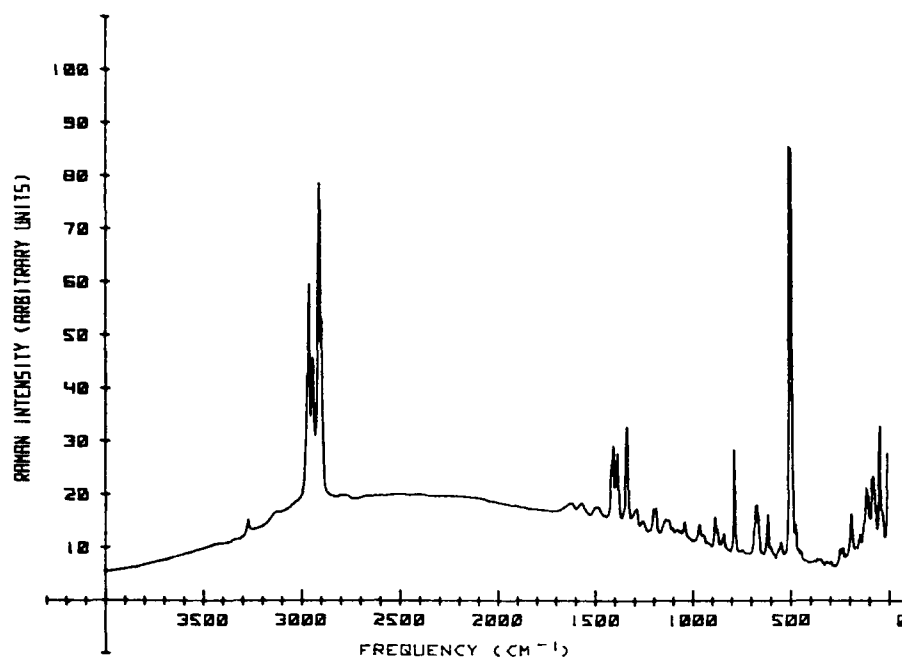


Figure B-7. Cystine (LG), 26 Apr 78.

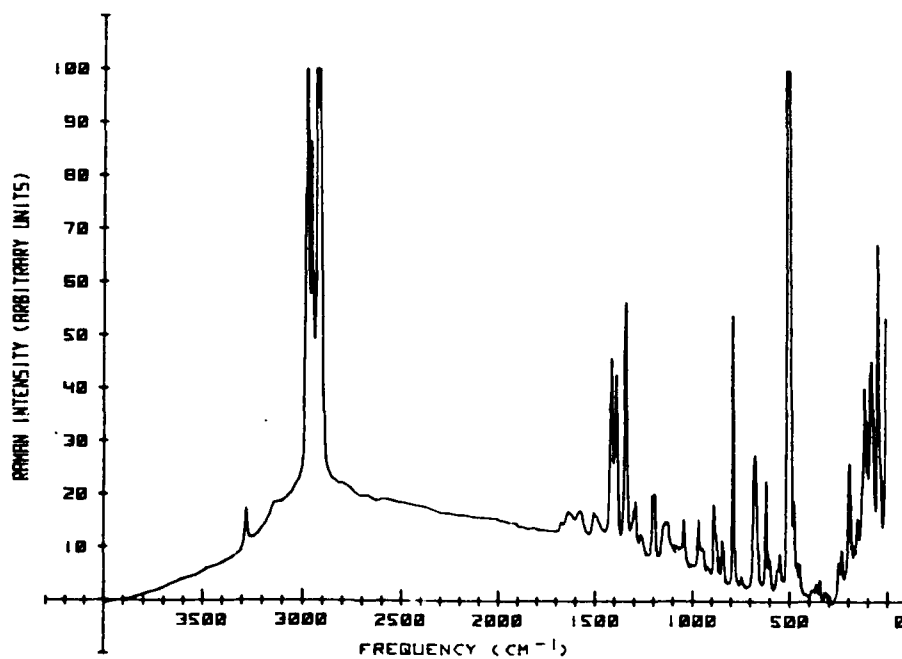


Figure B-8. Cystine (HG), 26 Apr 78.

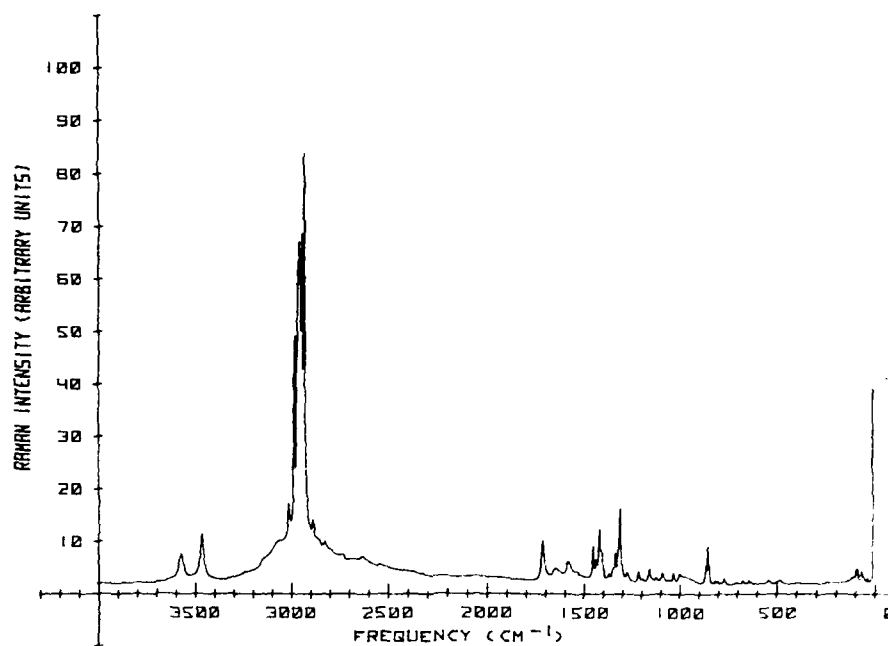


Figure B-9. Glutamic Acid (LG), 1 May 78.

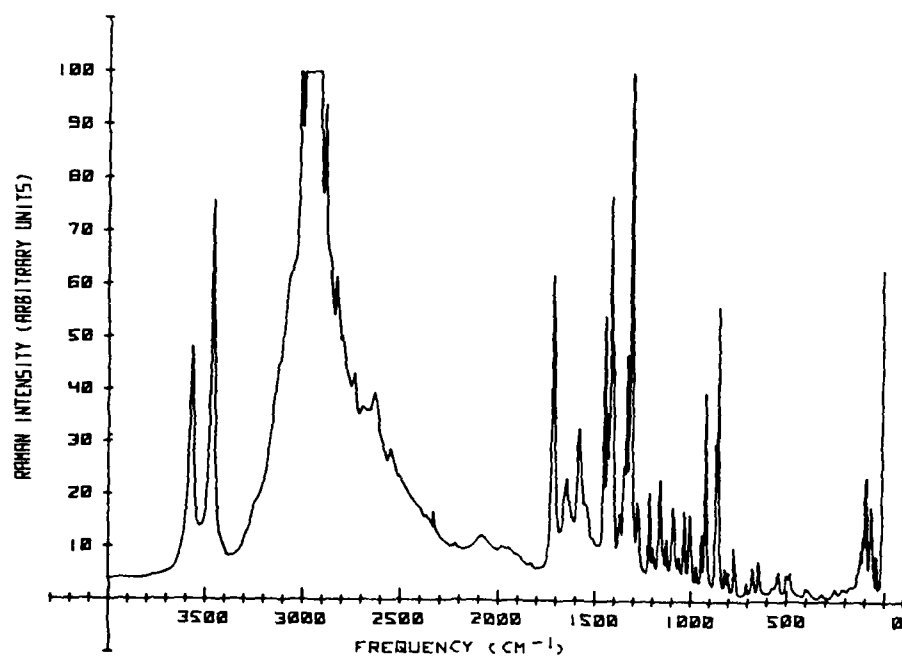


Figure B-10. Glutamic Acid (HG), 1 May 78.

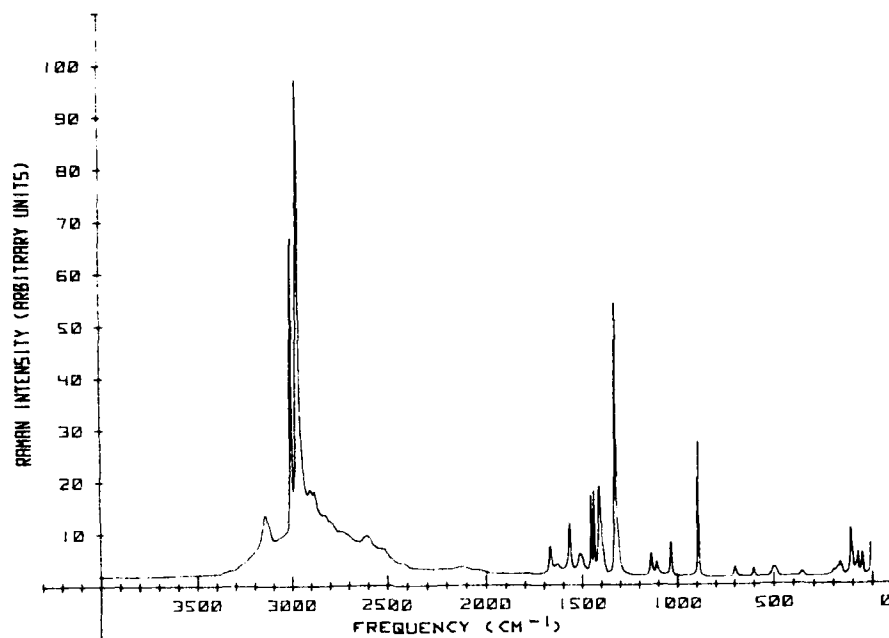


Figure B-11. Glycine (LG), 8 May 78.

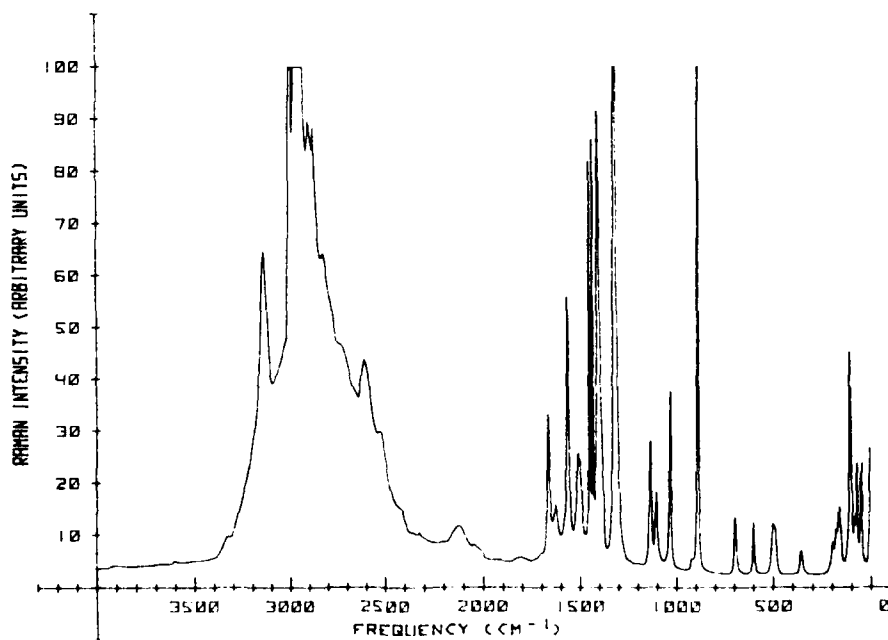


Figure B-12. Glycine (HG), 8 May 78.

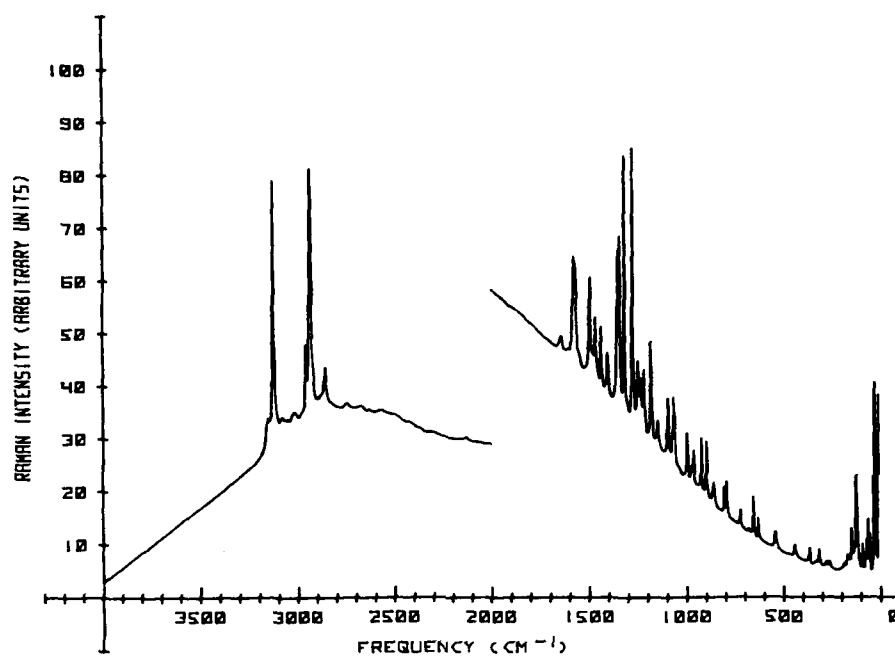


Figure B-13. Histidine, 28 Apr 78.

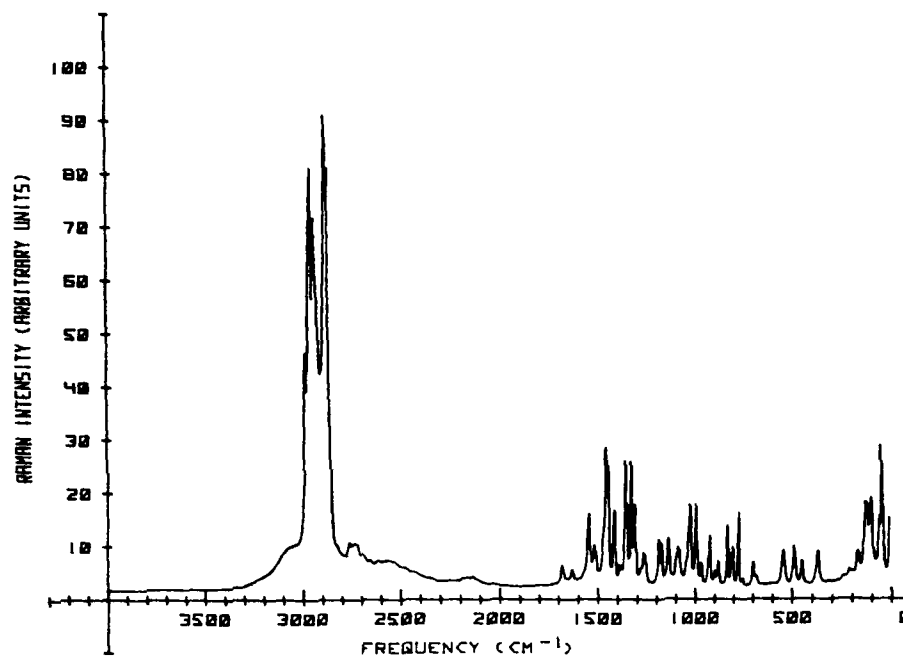


Figure B-14. Isoleucine (LG), 21 Apr 78.

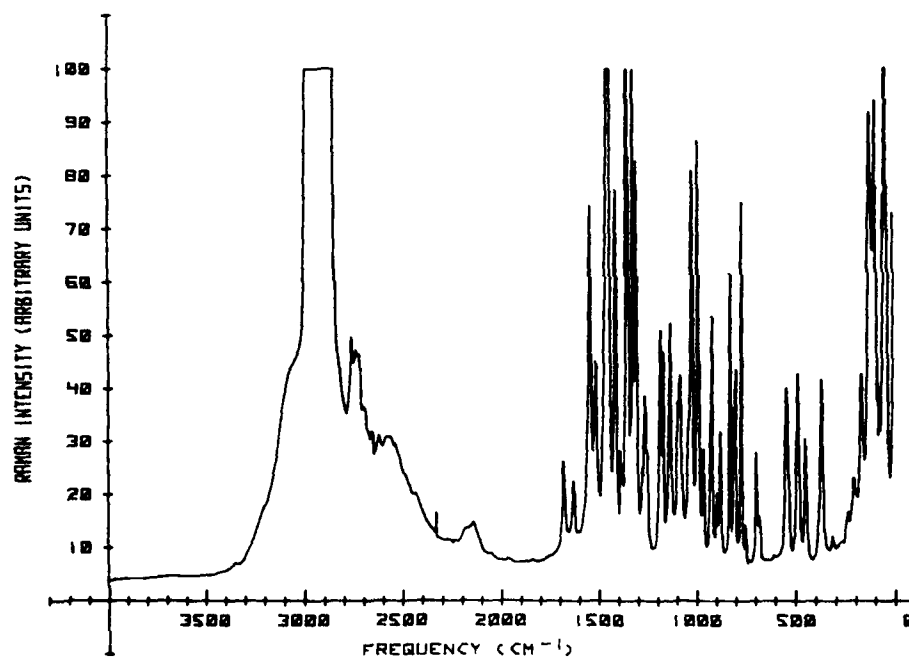


Figure B-15. Isoleucine (HG), 21 Apr 78.

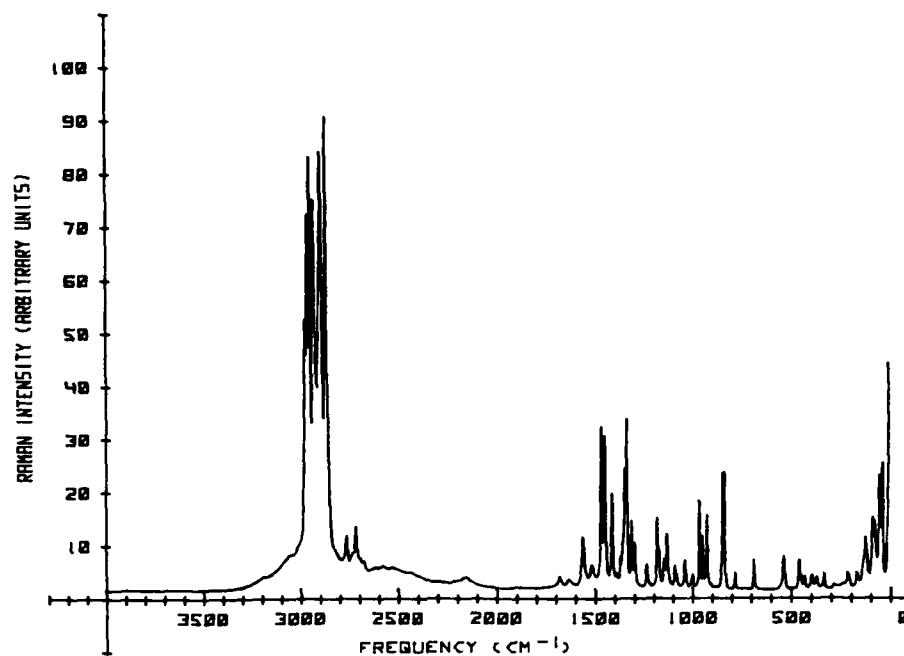


Figure B-16. Leucine (LG), 19 Apr 78.

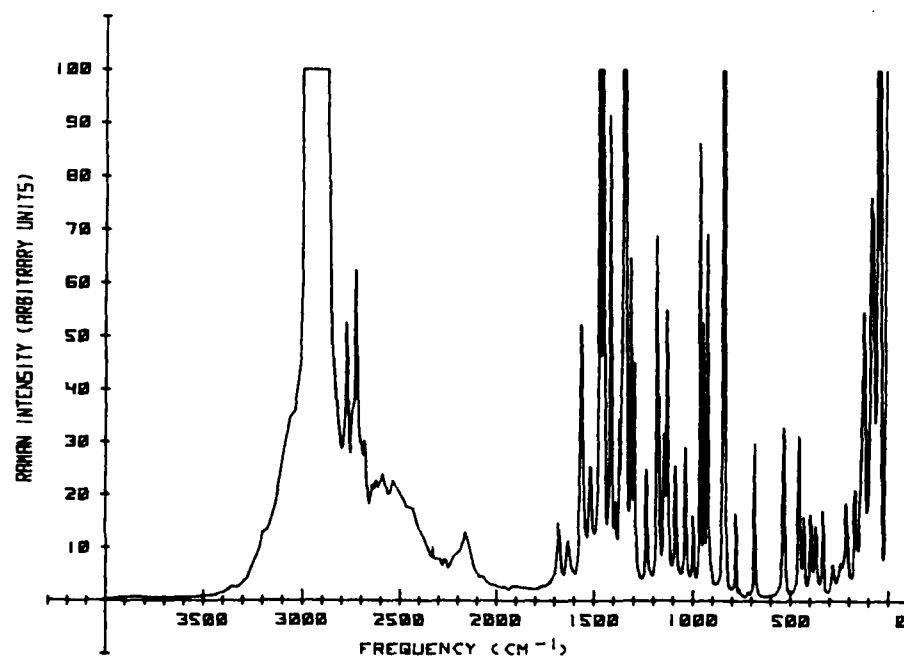


Figure B-17. Leucine (HG), 19 Apr 78.

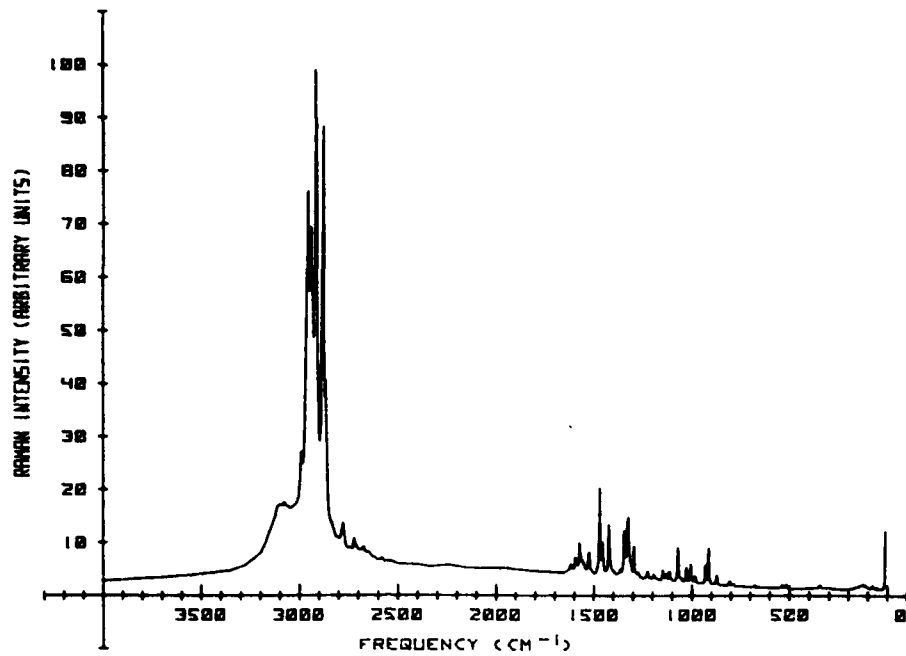


Figure B-18. Lysine (LG), 3 May 78.

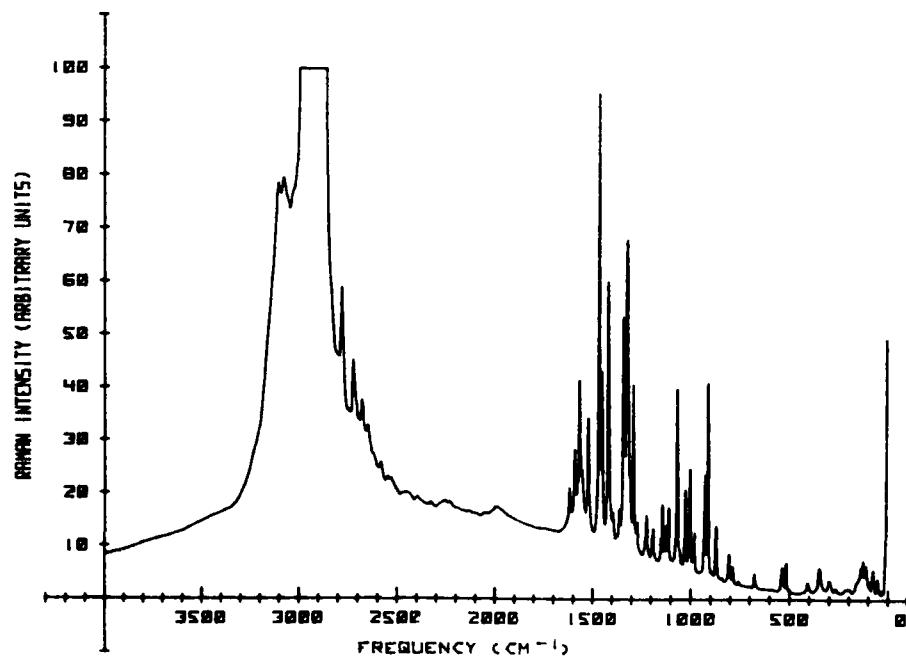


Figure B-19. Lysine (HG), 3 May 78.

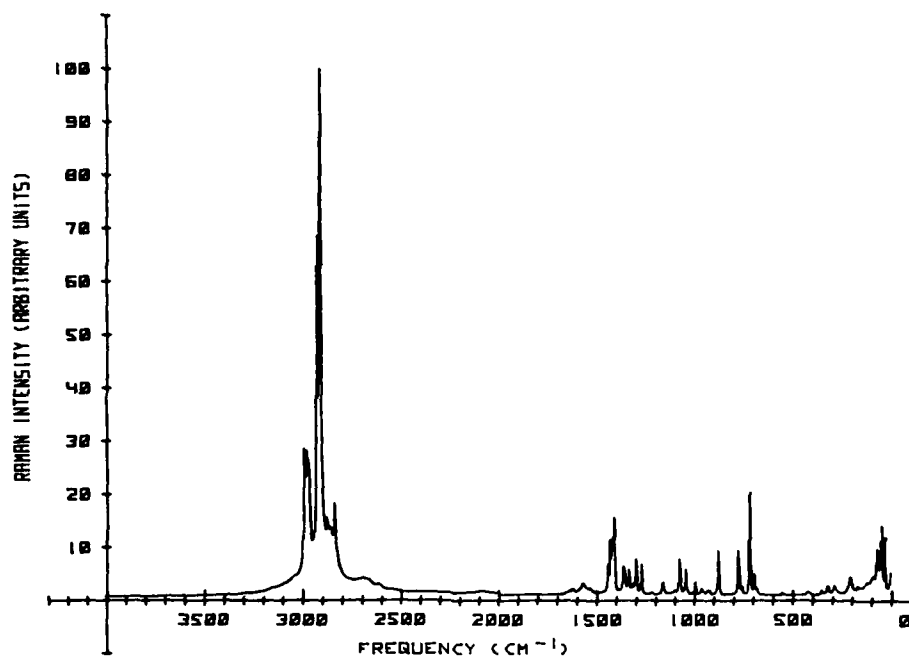


Figure B-20. Methionine (LG), 24 Mar 78.

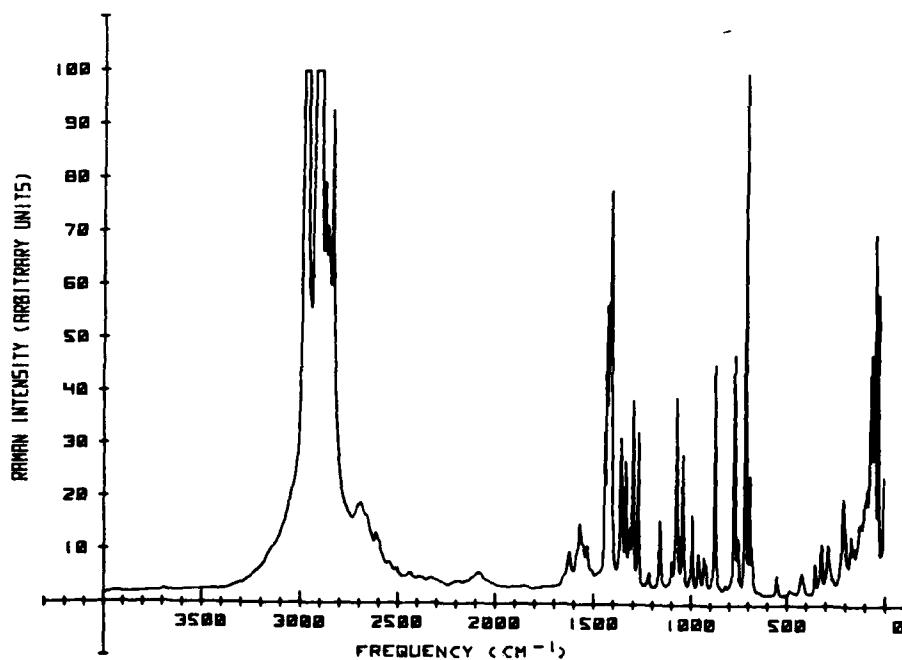


Figure B-21. Methionine (HG), 24 Mar 78.

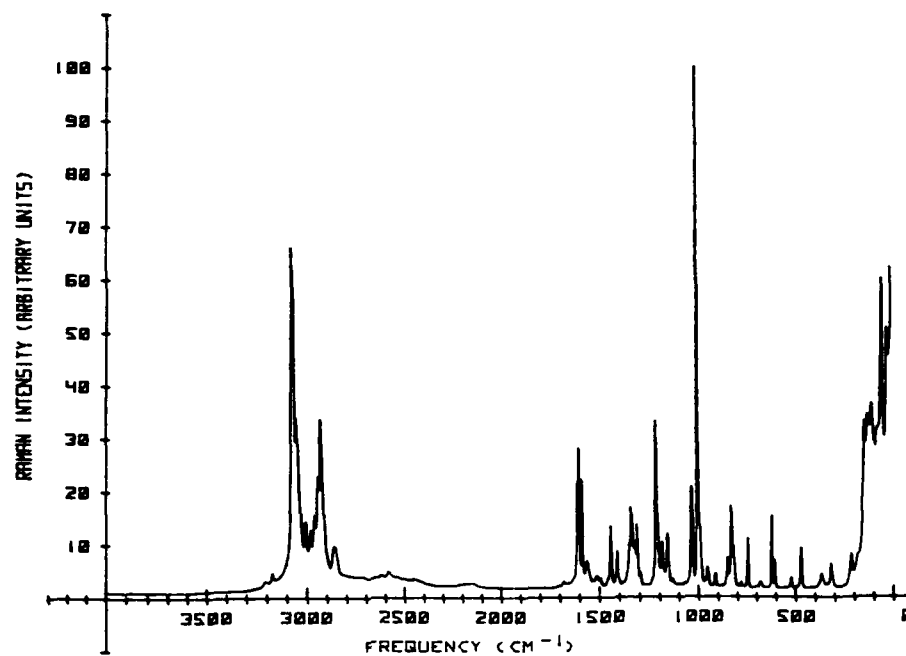


Figure B-22. Phenylalanine (LG), 24 Mar 78.

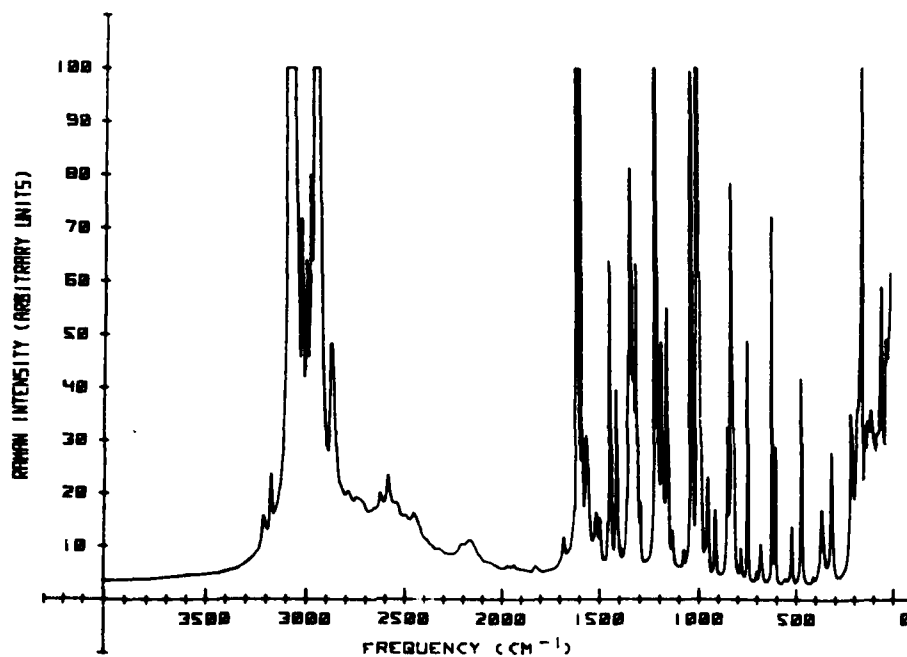


Figure B-23. Phenylalanine (HG), 24 Mar 78.

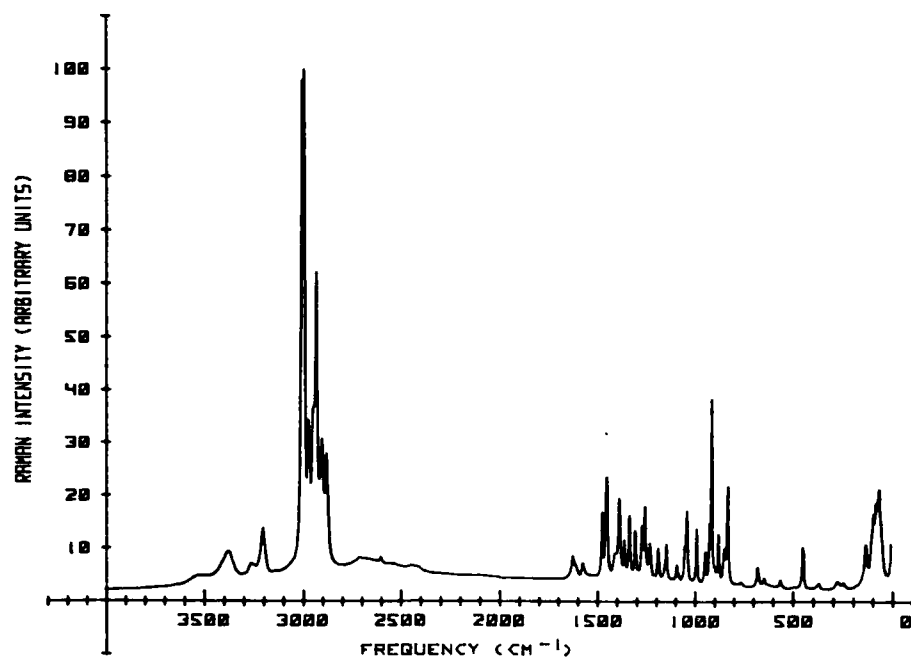


Figure B-24. Proline (LG), 26 Apr 78.

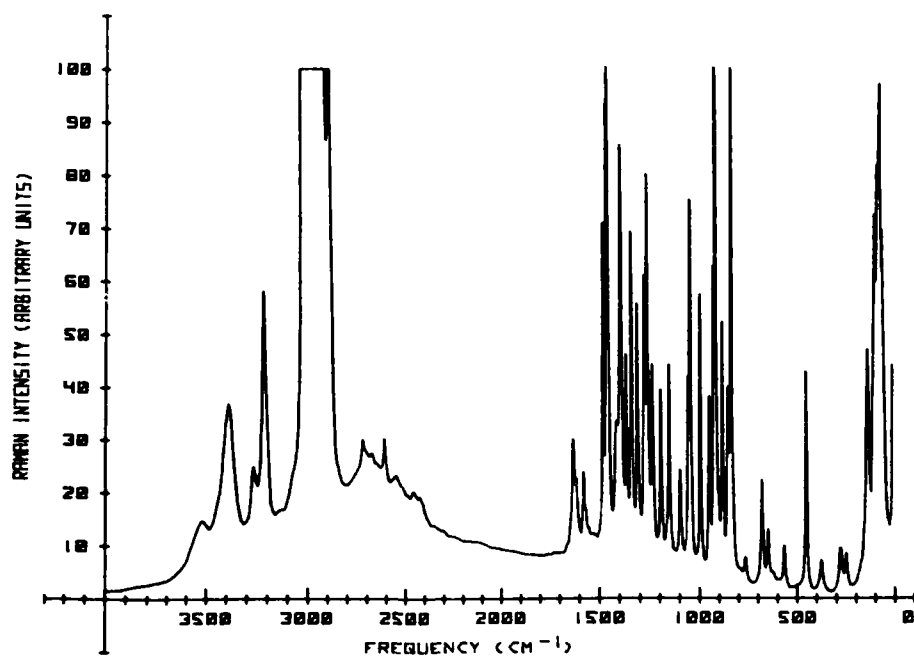


Figure B-25. Proline (HG), 27 Apr 78.

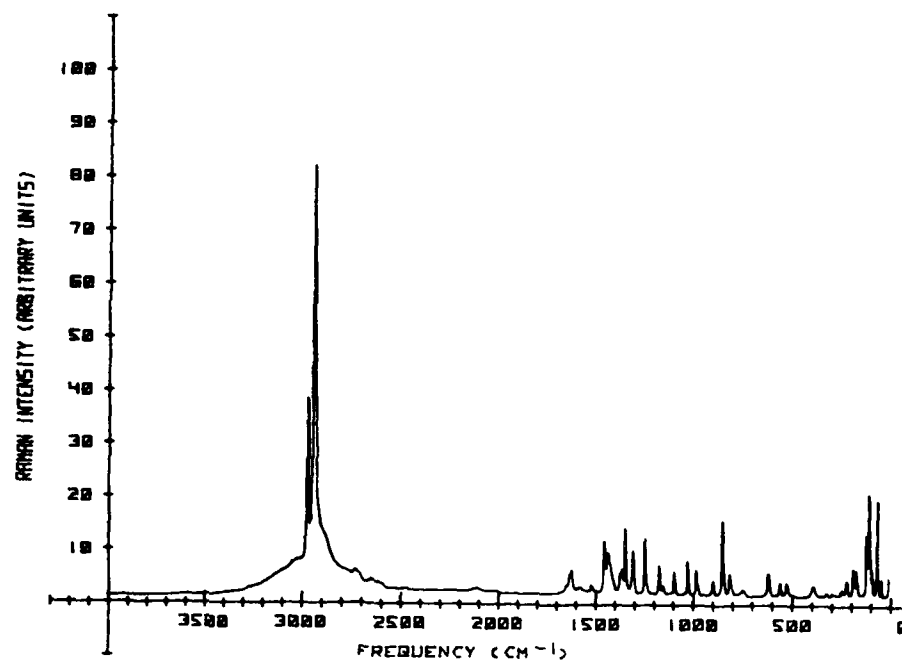


Figure B-26. Serine (LG), 20 Apr 78.

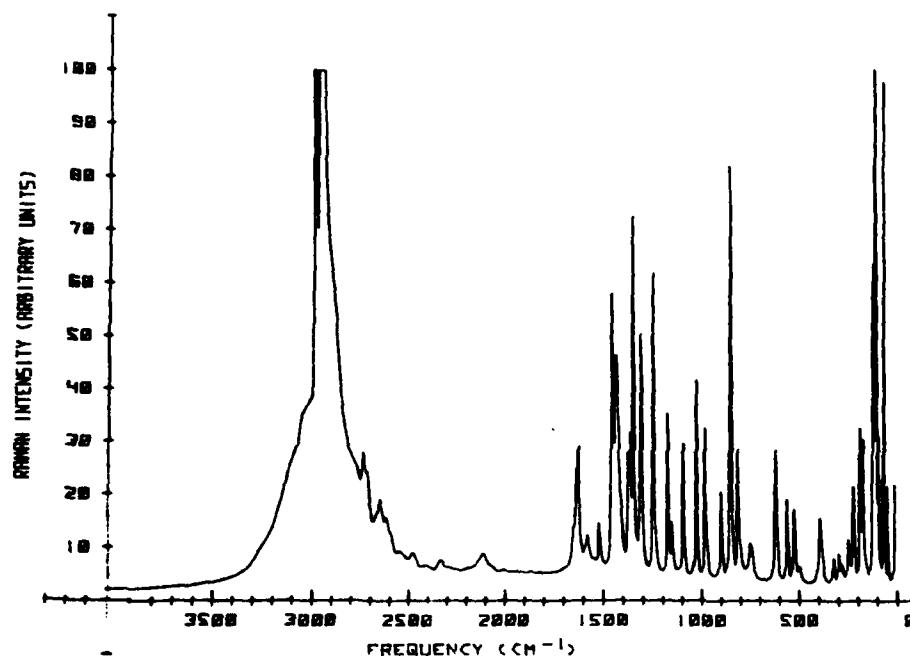


Figure B-27. Serine (HG), 20 Apr 78.

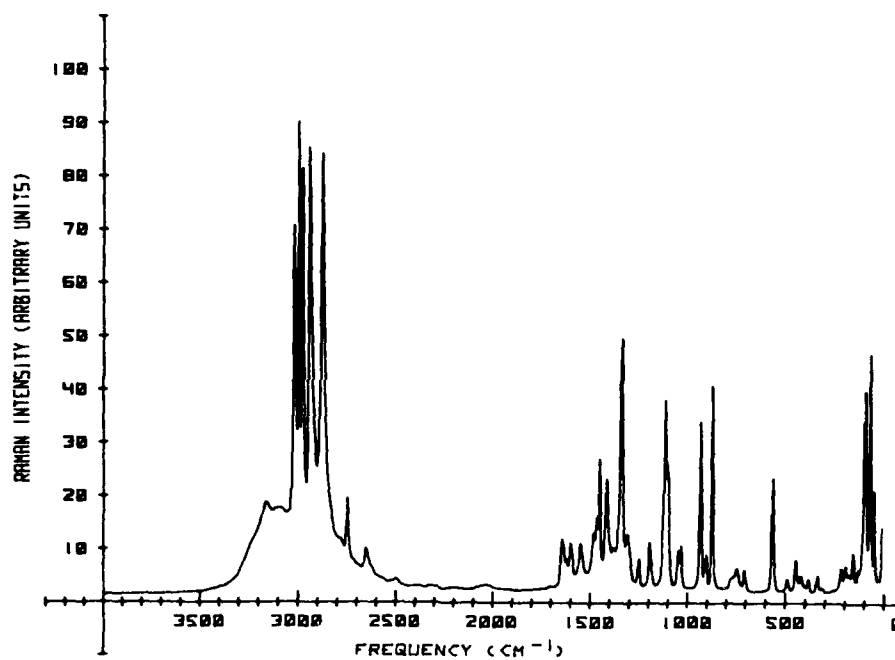


Figure B-28. Threonine (LG), 26 Apr 78.

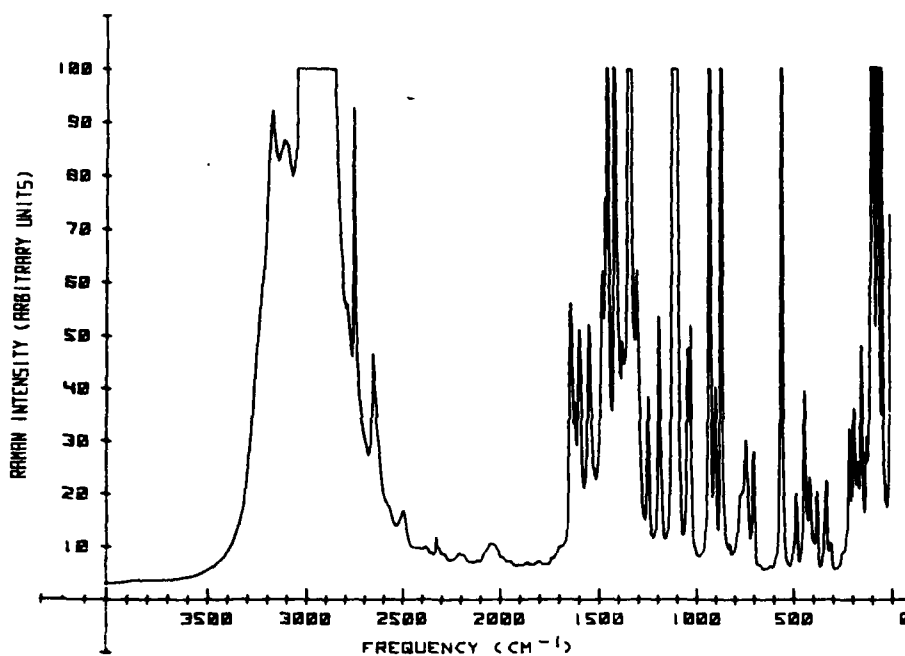


Figure B-29. Threonine (HG), 26 Apr 78.

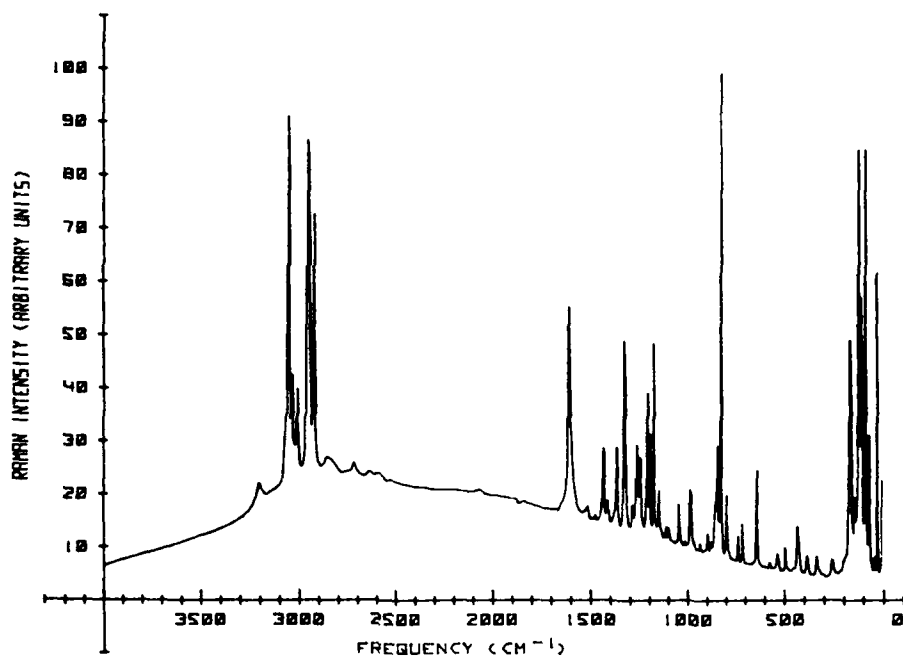


Figure B-30. Tyrosine (LG), 11 Apr 78.

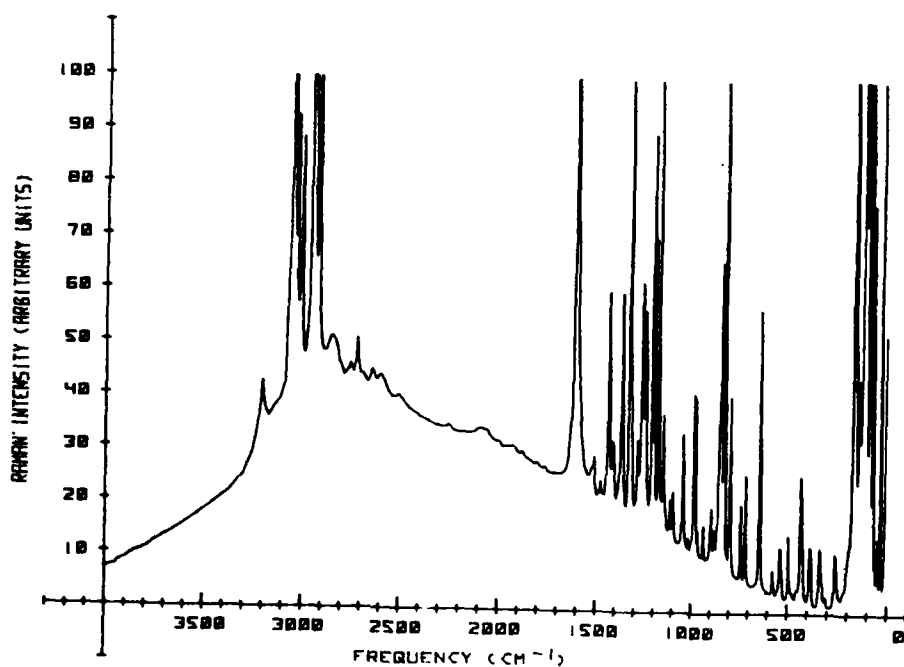


Figure B-31. Tyrosine (HG), 11 Apr 78.

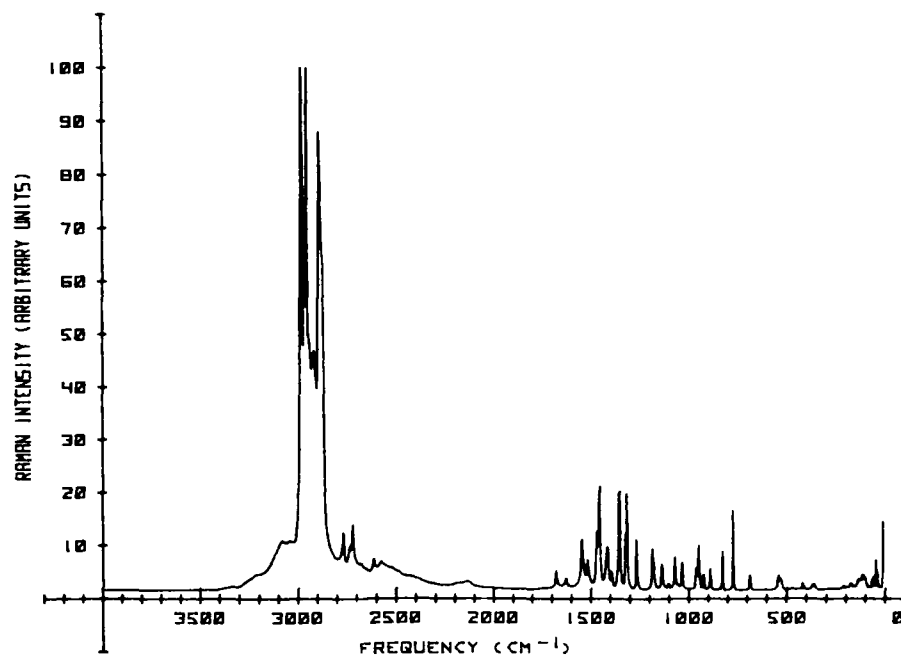


Figure B-32. Valine (LG), 2 May 78.

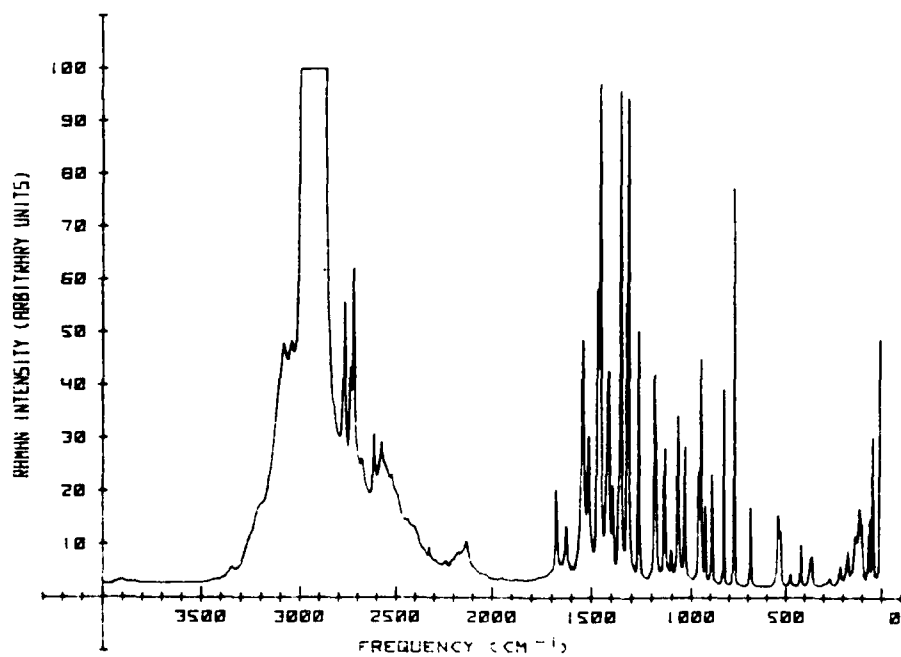


Figure B-33. Valine (HG), 2 May 78.